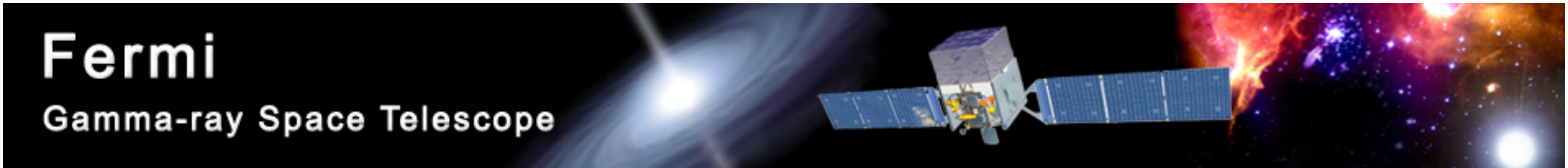

High Energy Emission in Pulsar Magnetospheres: Modeling in the FERMI Era

<u>Constantinos Kalapotharakos</u>
NASA, Goddard Space Flight Center

Collaborators:
Alice Harding (NASA GSFC)
Demos Kazanas (NASA GSFC)
Gabriele Brambilla (University of Milan, NASA GSFC)

Sixth International Fermi Symposium
Washington D.C., 9 – 13 November 2015

Outline

- FERMI (Success Requirements)
- Modeling γ-ray emission (CR)
- Comparison with FERMI observations
  Light curves and Spectral properties
- Successful Models - Understanding
- Summary

FERMI

Fermi has a catalytic role on the current modeling of the high energy emission in pulsar magnetospheres.

$N_p \longrightarrow \times 25 \qquad N_p > 160$ (117 in 2PC; Abdo et al. 2013)

Discovery Astronomy

established a number of trends and correlations

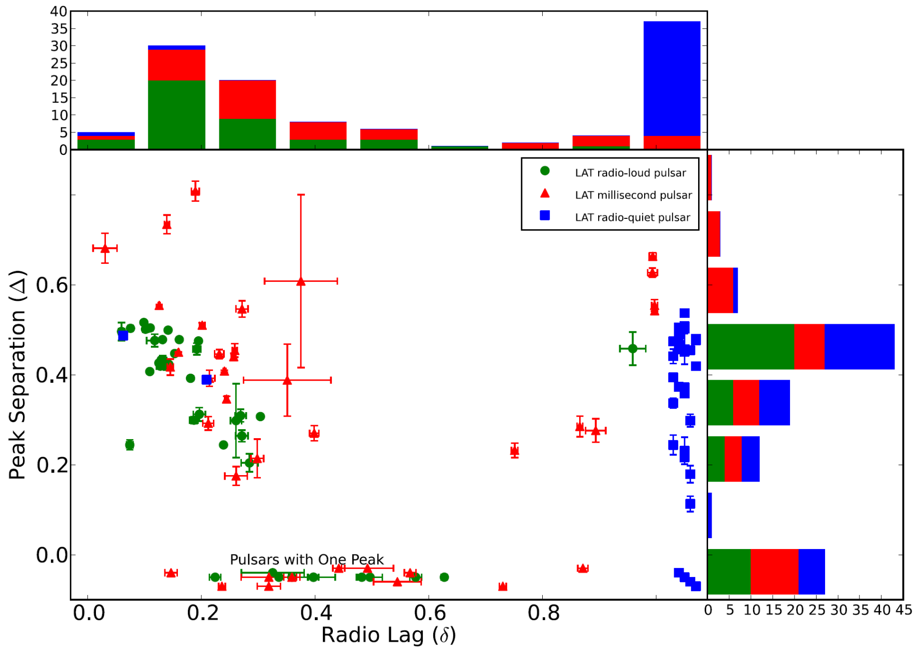

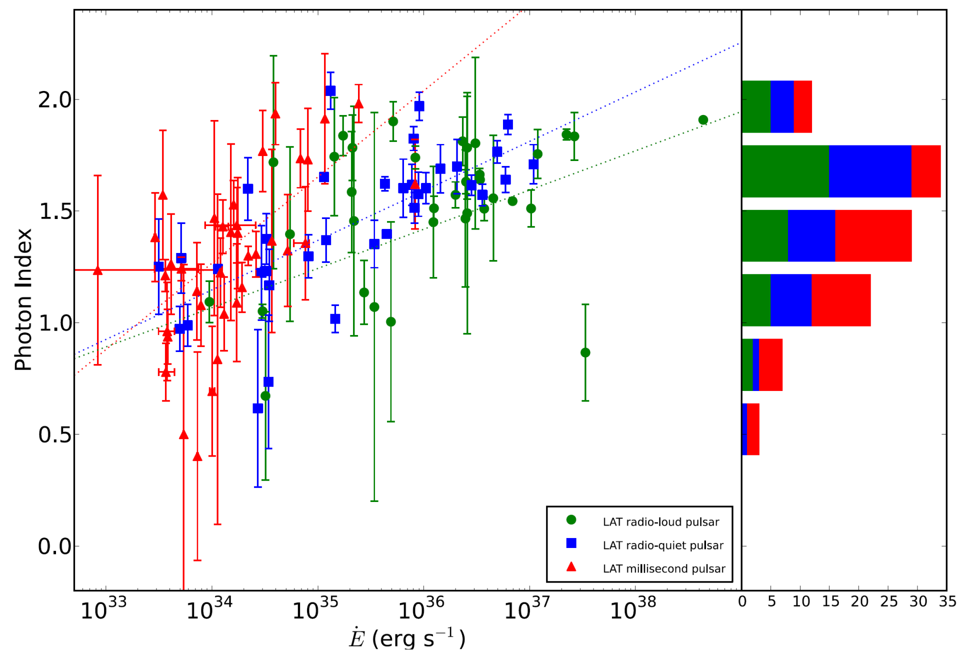

FERMI

Fermi has a catalytic role on the current modeling of the high energy emission in pulsar magnetospheres.

$$N_p \longrightarrow \times 25 \qquad N_p > 160 \text{ (117 in 2PC; Abdo et al. 2013)}$$

Discovery Astronomy

established a number of trends and correlations

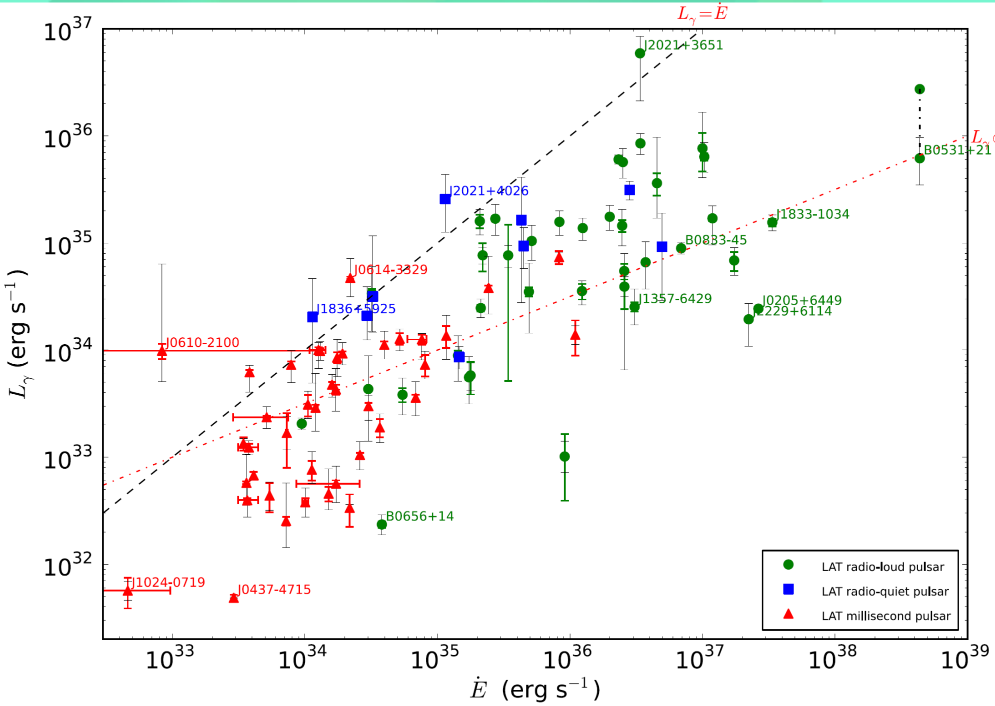

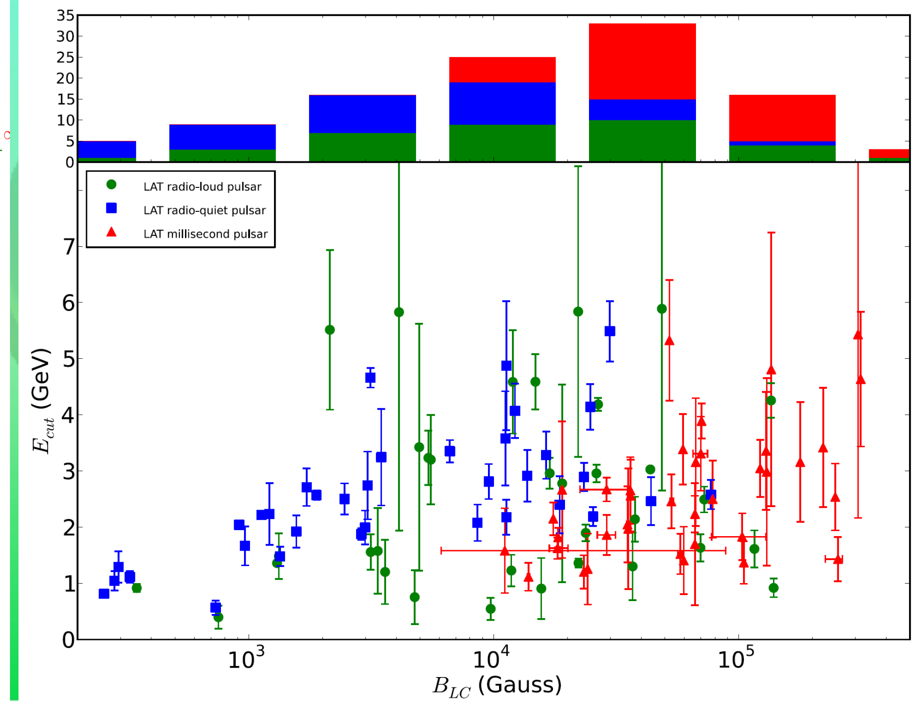

FERMI

Fermi has a catalytic role on the current modeling of the high energy emission in pulsar magnetospheres.

$N_p \longrightarrow \times 25 \qquad N_p > 160$ (117 in 2PC; Abdo et al. 2013)

Fermi provides not only **phase-averaged** spectra but also **phase-resolved** for a dozen of pulsars

Vela

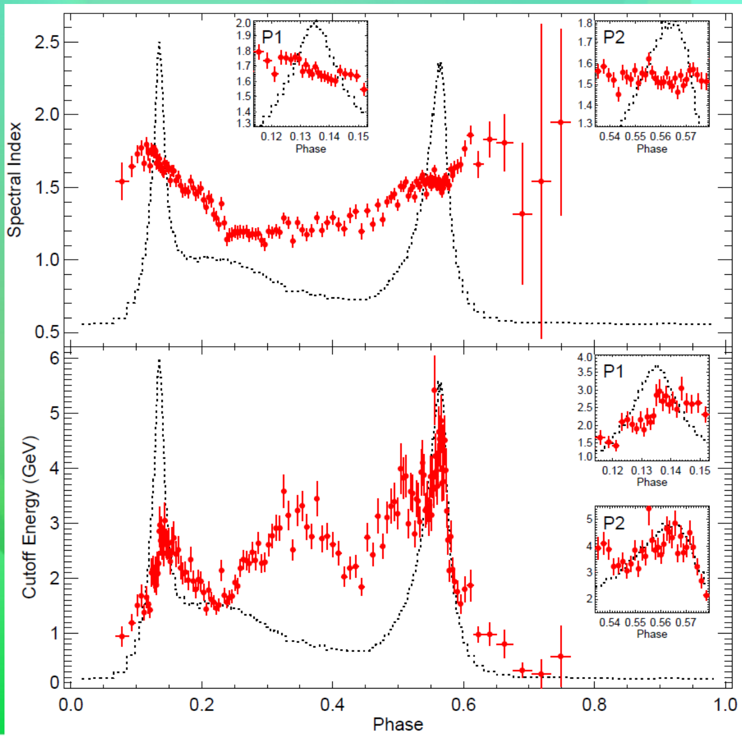

Geminga

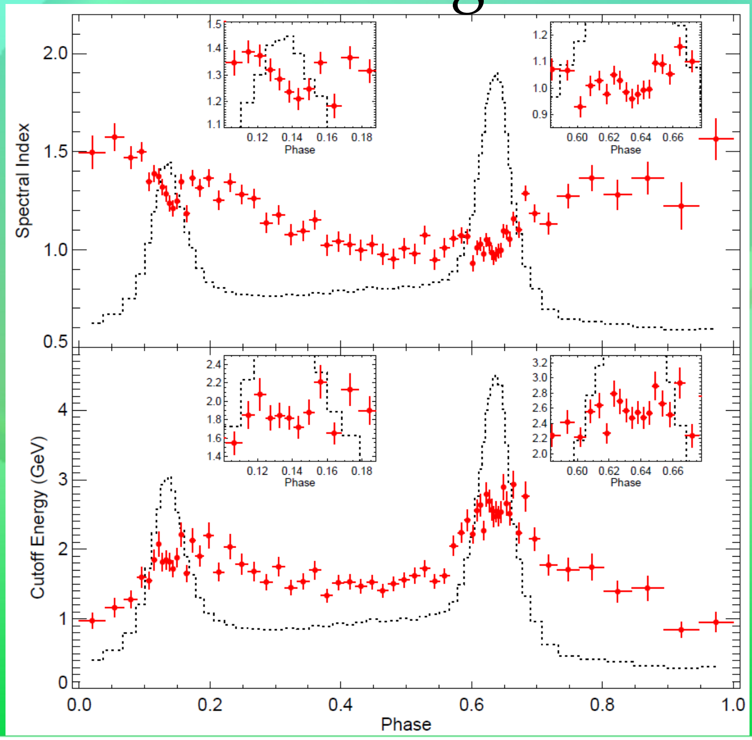

FERMI

Fermi has a catalytic role on the current modeling of the high energy emission in pulsar magnetospheres.

$N_p \longrightarrow \times 25 \quad N_p > 160$ (117 in 2PC; Abdo et al. 2013)

Fermi provides not only **phase-averaged** spectra but also **phase-resolved** for a dozen of pulsars

A successful high energy emission model should be able to reproduce the observed pulsar light curve and spectral properties

Eventually, a physical justification consistent with the microphysics is required

(FFE) solutions

Contopoulos, Kazanas & Fendt (1999)
(Aligned Rotator)

Spitkovsky (2006) (Oblique Rotator)

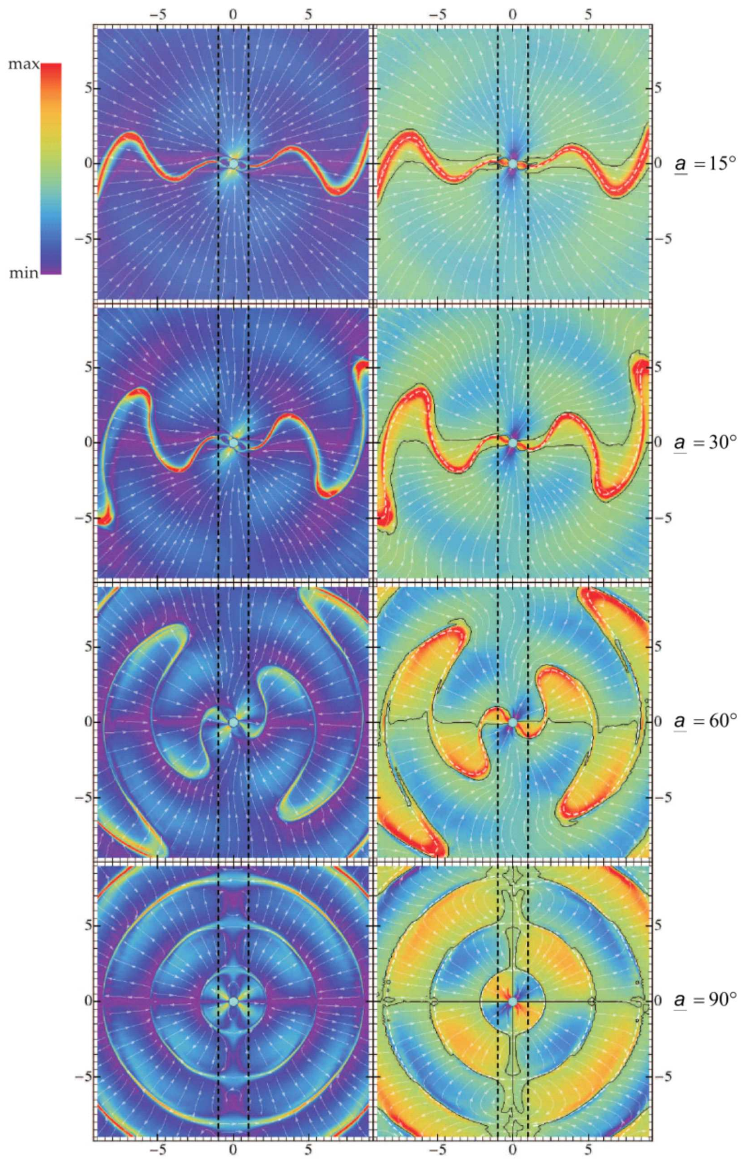

$$J = \rho_e \frac{E \times B}{B^2} + \frac{1}{4\pi} \frac{\left(B \cdot \nabla \times B - E \cdot \nabla \times E\right)}{B^2} B$$

Gruzinov (1999)

$$E \cdot B = 0$$ Ideal condition

Kalapotharakos & Contopoulos (2009)
Contopoulos & Kalapotharakos (2010)
Kalapotharakos, Contopoulos & Kazanas (2012)

(FFE) solutions

Contopoulos, Kazanas & Fendt (1999)
(Aligned Rotator)

Spitkovsky (2006) (Oblique Rotator)

Bogovalov (1999)

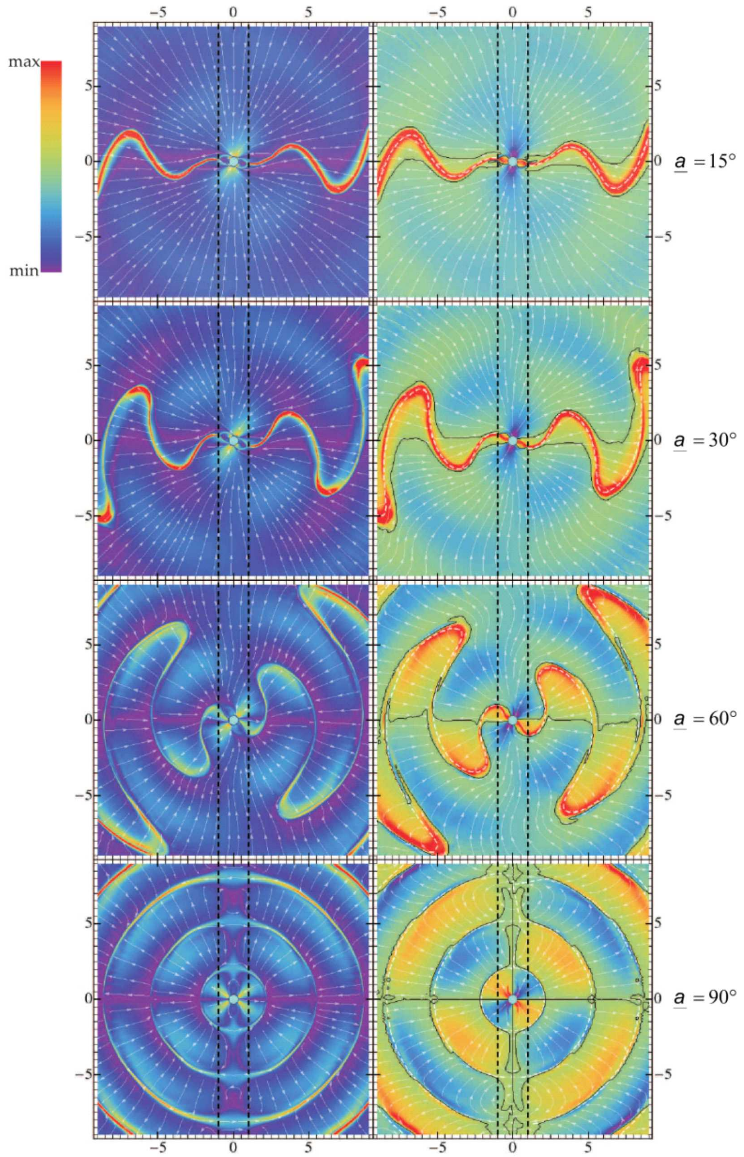

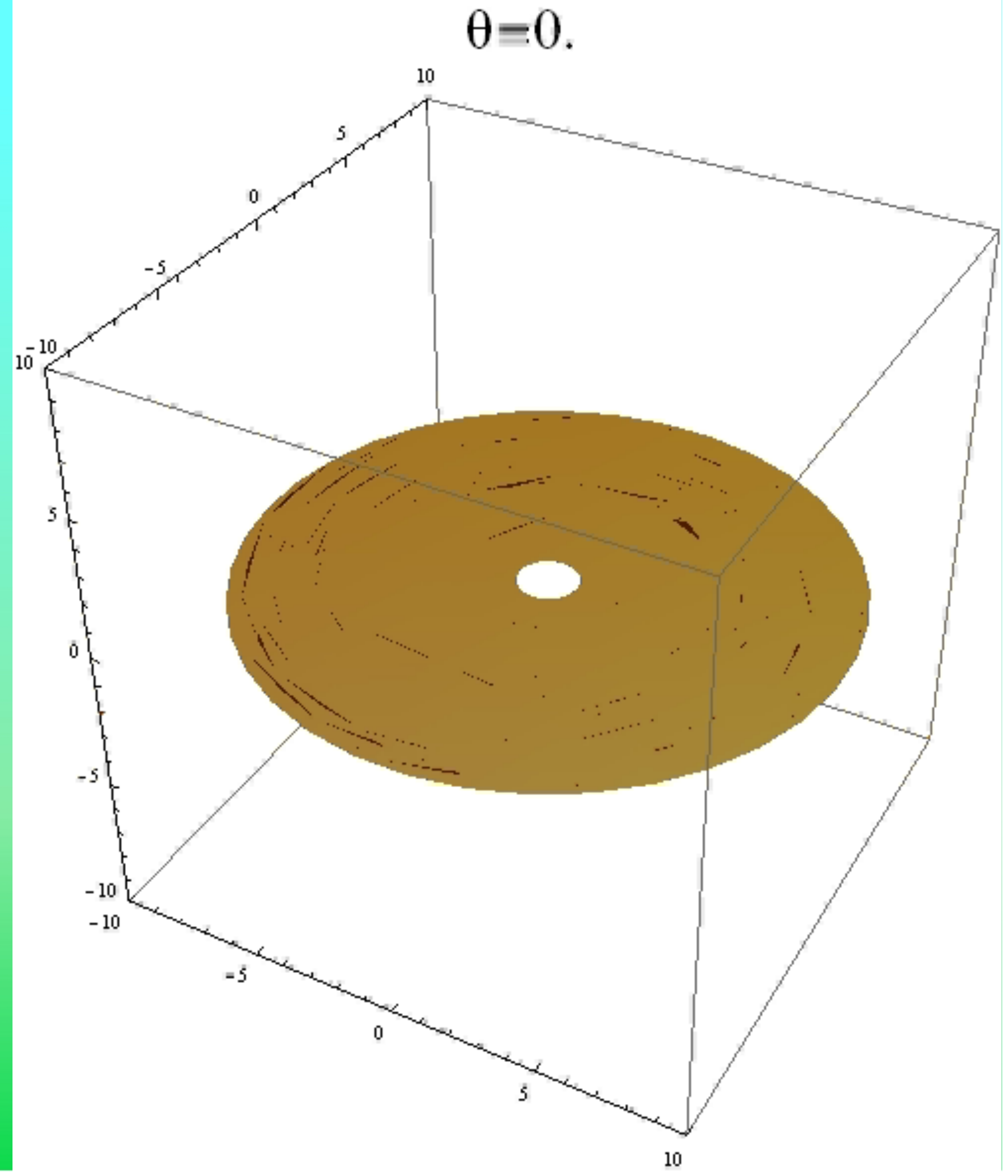

Something is missing

Force-Free solutions may be a good indicator of the magnetic field structure

But…

they say nothing about the necessary accelerating electric fields

$$E_{\text{accel}} = 0$$

Dissipative Solutions

$$\mathbf{J} = c\rho\frac{\mathbf{E}\times\mathbf{B}}{B^2} + \frac{c}{4\pi}\frac{\mathbf{B}\cdot\nabla\times\mathbf{B} - \mathbf{E}\cdot\nabla\times\mathbf{E}}{B^2}\mathbf{B}$$

FFE

$$\mathbf{J} = c\rho\frac{\mathbf{E}\times\mathbf{B}}{E_0^2 + B^2} + \sigma E_{\parallel}$$

Kalapotharakos et al. (2012, 2014)

$$\mathbf{J} = \frac{c\rho\mathbf{E}\times\mathbf{B} + (c^2\rho^2 + \gamma^2\sigma^2 E_0^2)^{1/2}(B_0\mathbf{B} + E_0\mathbf{E})}{B^2 + E_0^2}$$

Gruzinov (2007, 2008)

$$\mathbf{J} = \frac{c\rho\mathbf{E}\times\mathbf{B} + \gamma\sigma(B_0\mathbf{B} + E_0\mathbf{E})}{B^2 + E_0^2}$$

Li et al. (2012)

$$\sigma: \quad 0 \longrightarrow \infty$$

$$\text{VRD} \longrightarrow \text{FFE}$$

Dissipative Solutions

Very high σ
near FFE

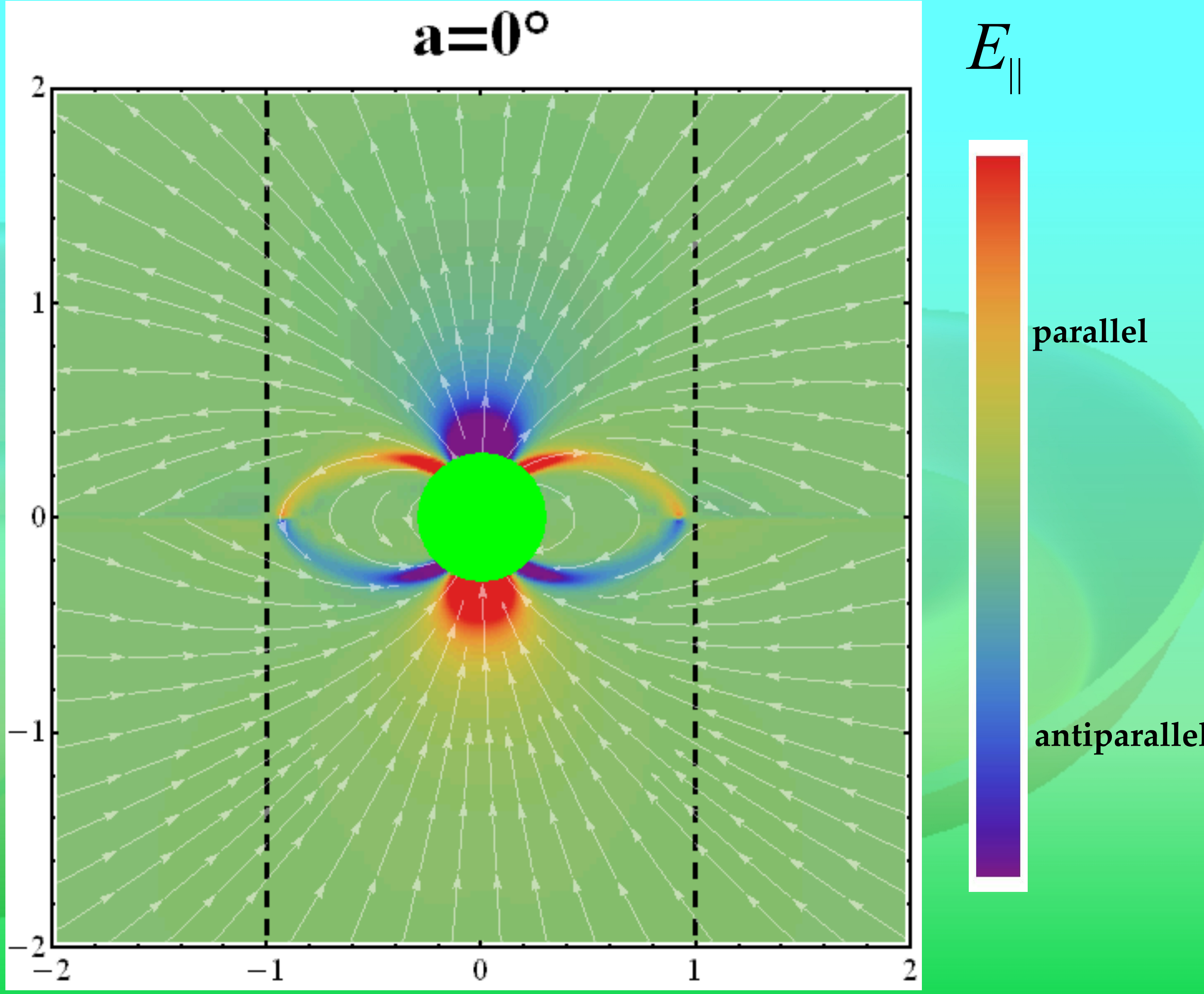

Modeling γ-ray emission

curvature radiation

We consider trajectories

$$\mathbf{v} = \frac{\mathbf{E}\times\mathbf{B} \pm (B_0\mathbf{B} + E_0\mathbf{E})}{B^2 + E_0^2}$$

$v = c$

motion outwards

Aristotelian Electrodynamics
Gruzinov (2013)

$$\frac{d\gamma}{dt} = \frac{q_e c E_{||}}{m_e c^2} - \frac{2}{3}\frac{q_e^2\gamma^4}{R_{cr}^2 m_e c}$$

Curvature Radiation

Uniform conductivity (σ)

σ: **Low** → **High**

Inner Magnetosphere → **Outer Magnetosphere Current Sheet**

Models vs Fermi

light curves

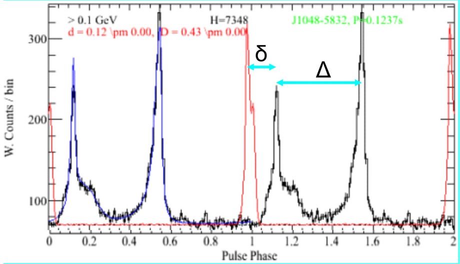

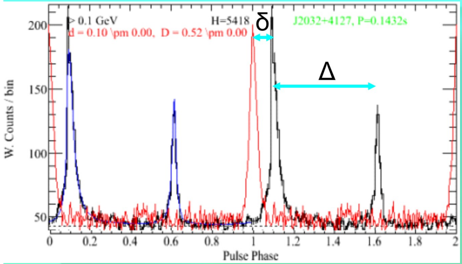

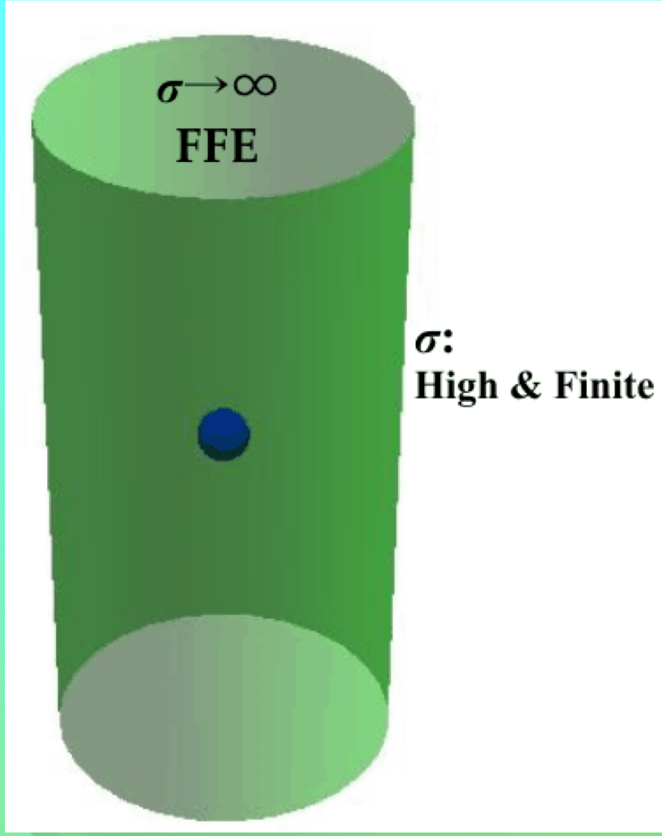

radio-lag (δ)
vs
peak-separation (Δ)

Kalapotharakos et al. (2014)

FIDO Models
(FFE Inside the Light-Cylinder,
Dissipative Outside the Light Cylinder)

Models vs Fermi
light curves

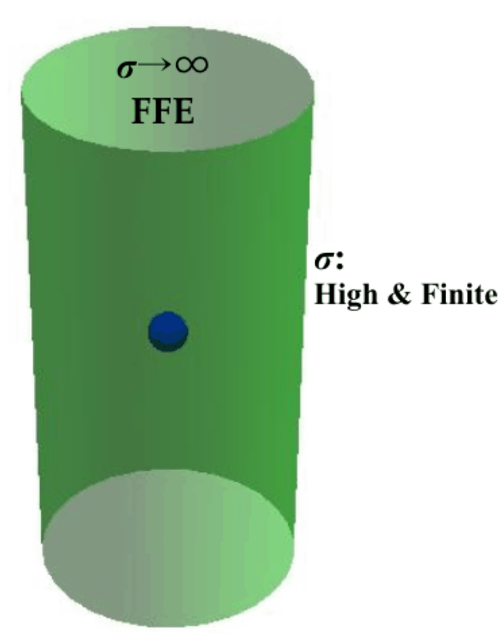

The black points are the standard pulsars observed by Fermi

Kalapotharakos et al. (2014)

FFE Inside Dissipative Outside (FIDO) model

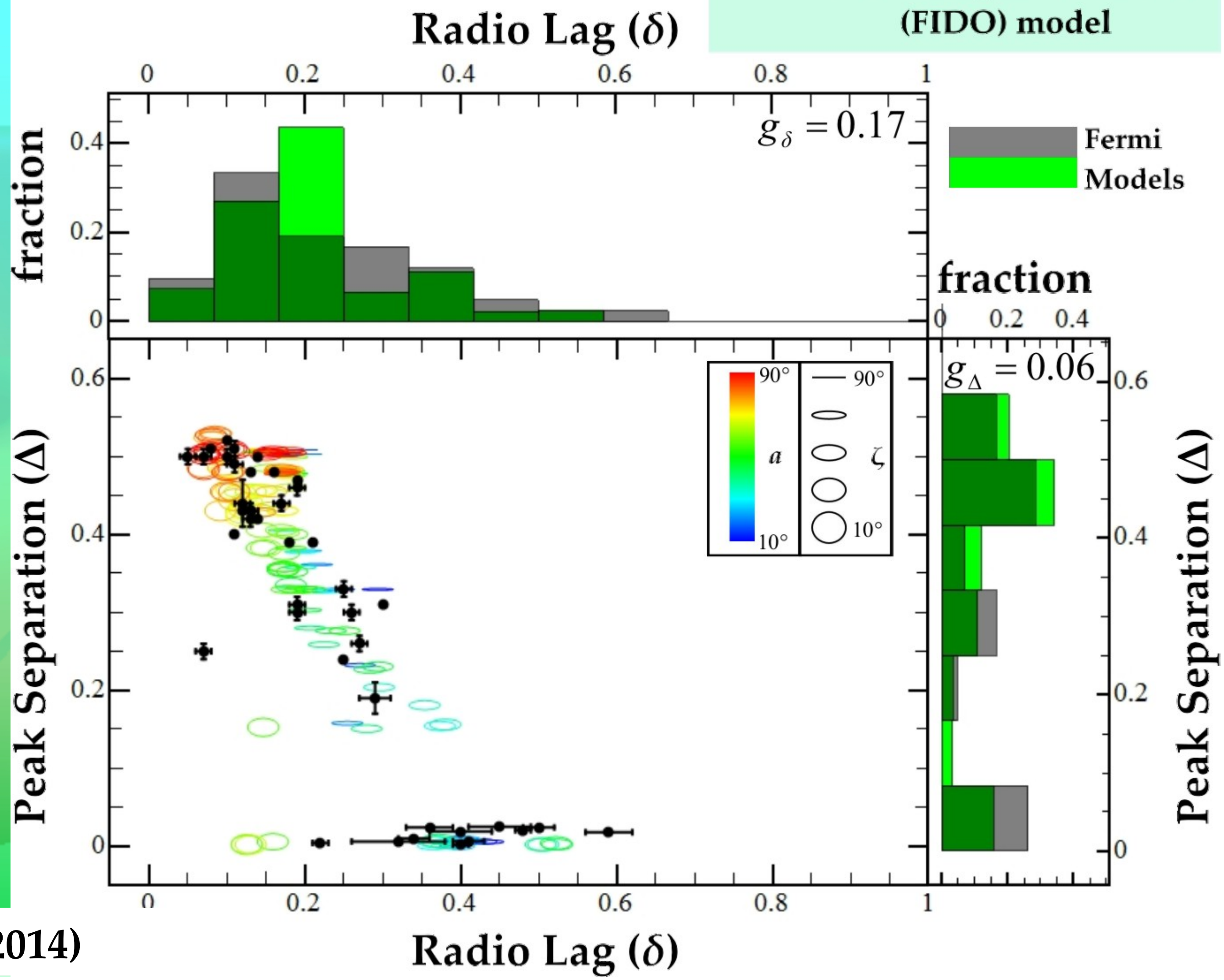

Models vs Fermi
light curves

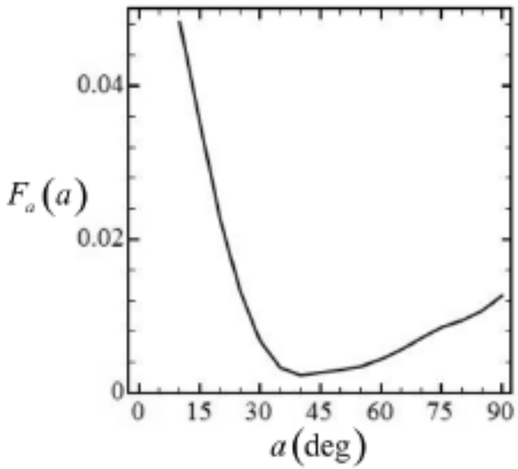

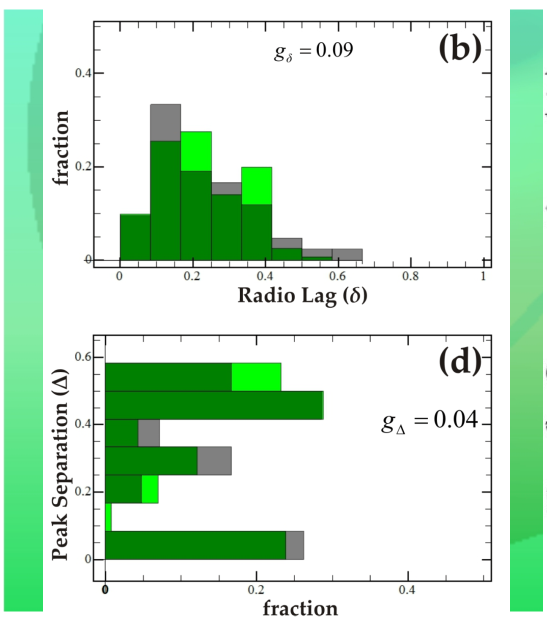

Kalapotharakos et al. (2014)

FFE Inside Dissipative Outside (FIDO) model

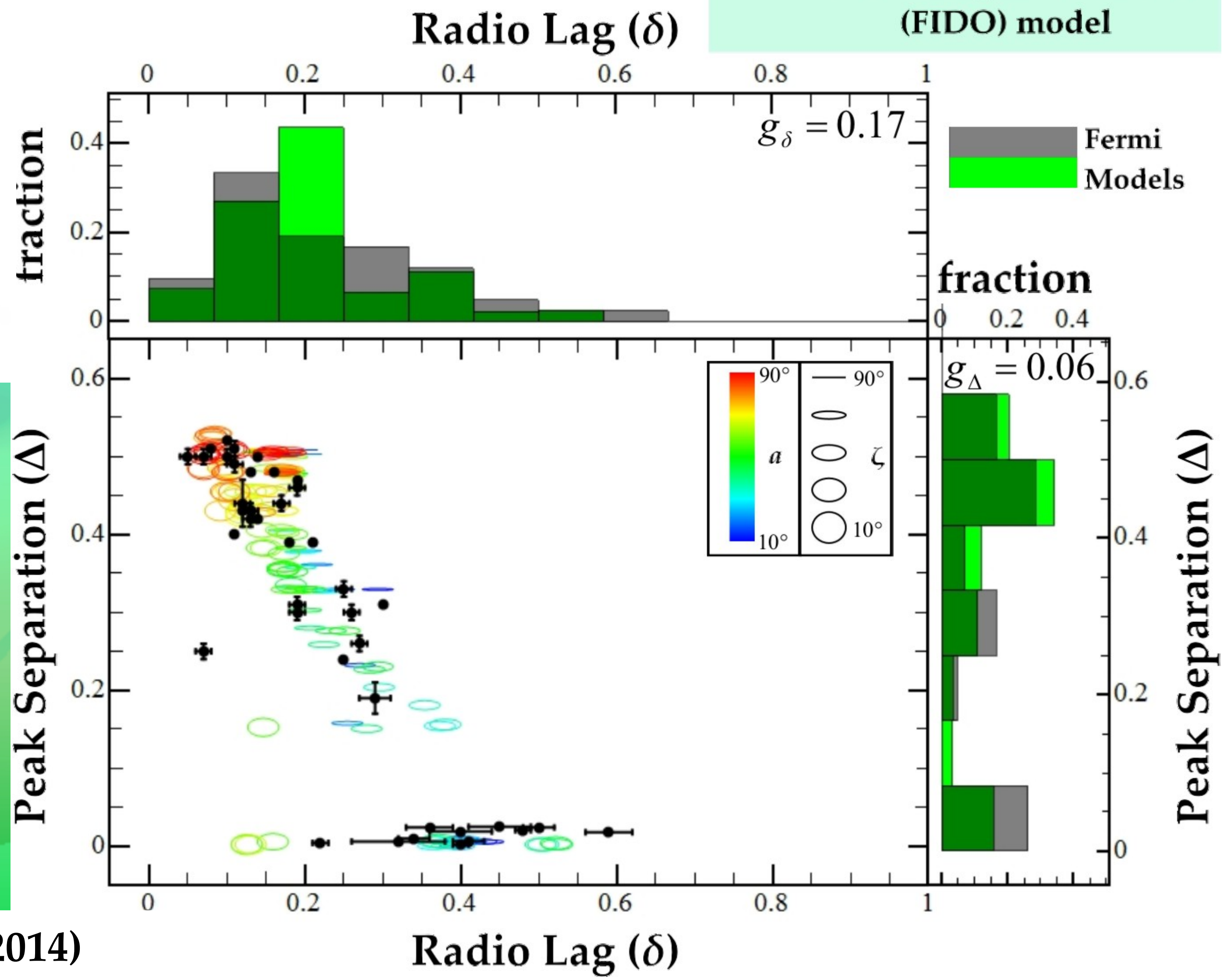

Models vs Fermi

light curves

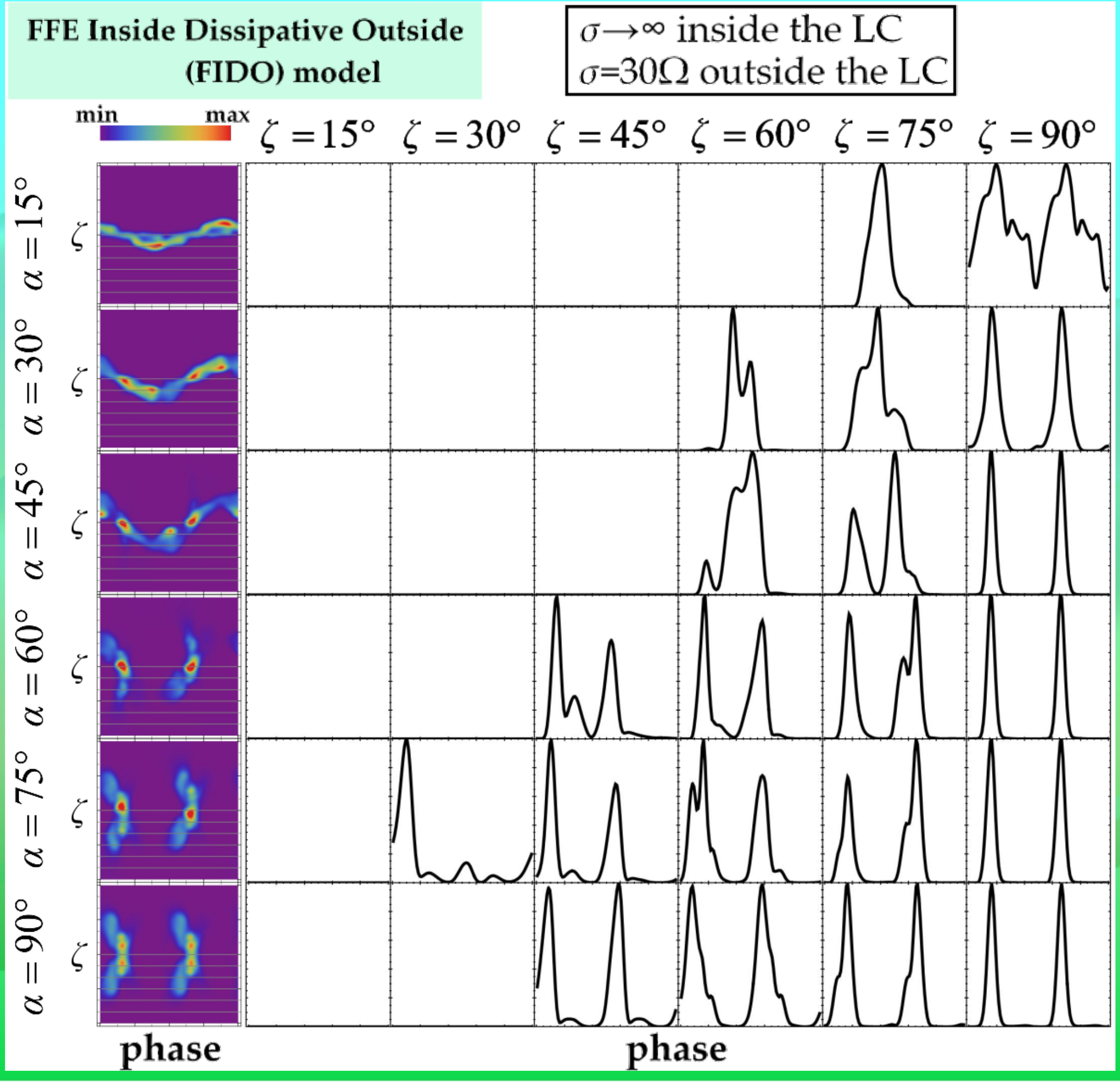

FIDO model - Spectral properties

The FIDO model allows the calculation of the phase-averaged, phase-resolved spectra and the calculation of the total γ-ray luminosity.

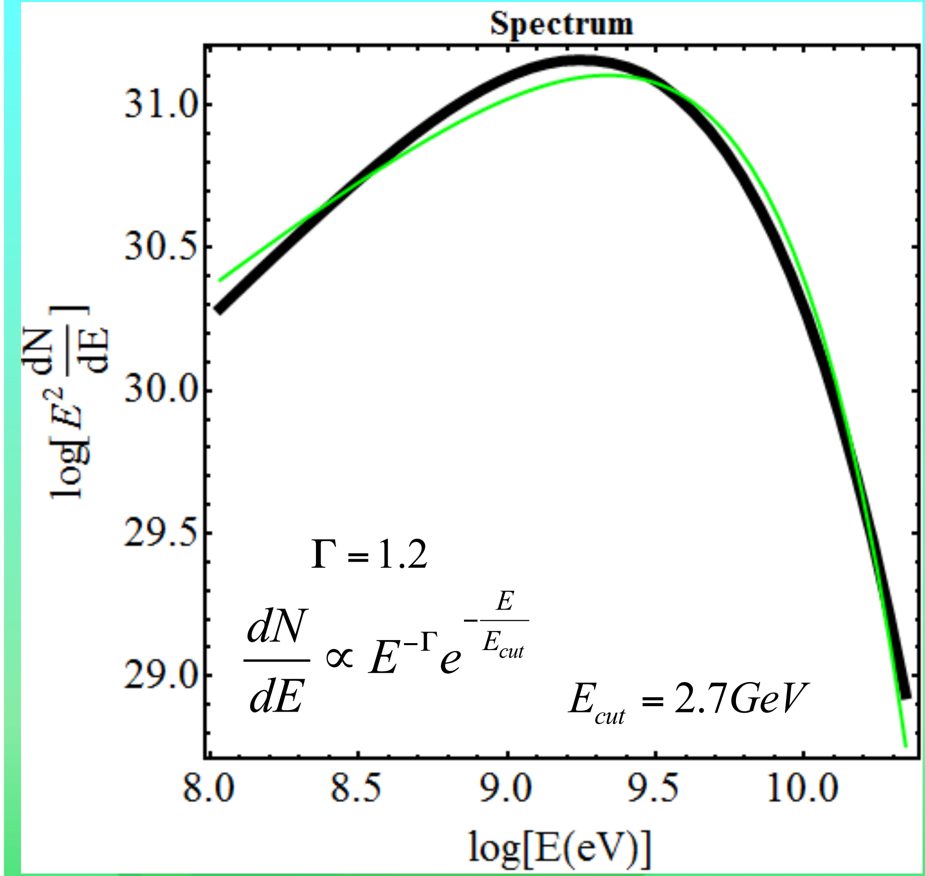

Broad range of σ values.

Low σ values everywhere applied outside the LC destroy the FF field structure.

We have explored models with low σ only near the open field boundary, extending outside the LC along the current sheet.

FIDO model - Spectral properties

The FIDO model allows the calculation of the phase-averaged, phase-resolved spectra and the calculation of the total γ-ray luminosity.

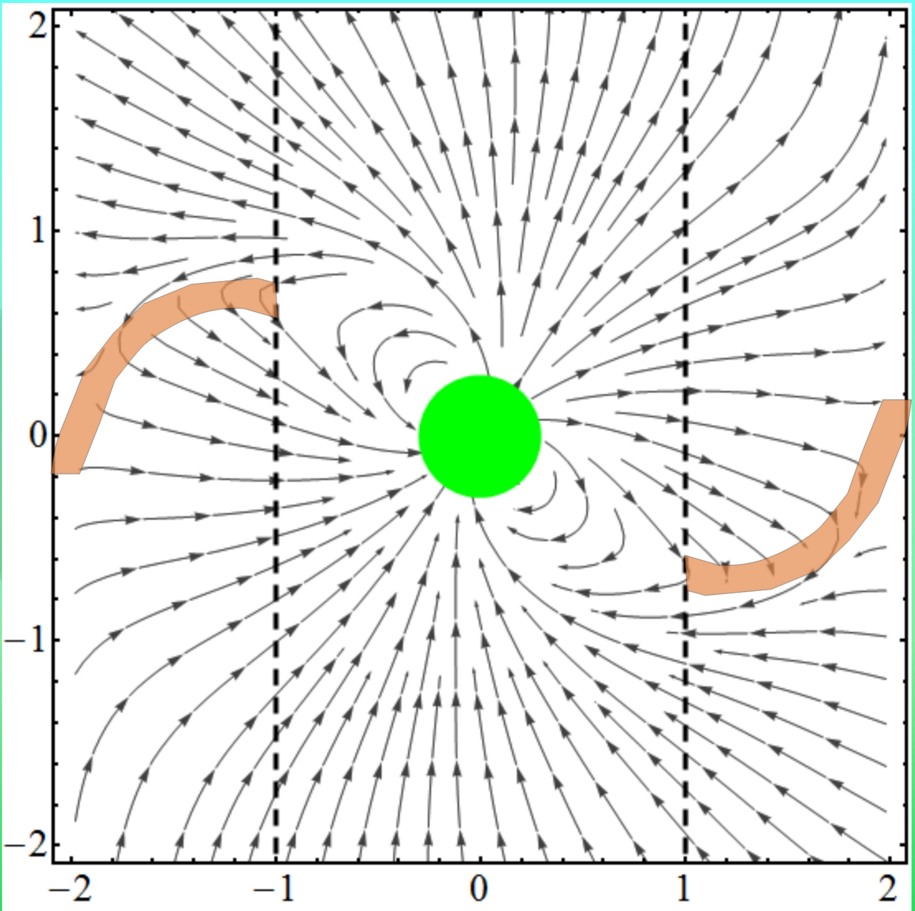

Broad range of σ values.

Low σ values everywhere applied outside the LC destroy the FF field structure.

We have explored models with low σ only near the open field boundary, extending outside the LC along the current sheet.

FIDO model - Spectral properties

The FIDO model allows the calculation of the phase-averaged, phase-resolved spectra and the calculation of the total γ-ray luminosity.

We ran series of models with different combinations for <u>*P*, *B*, and *σ*</u> values that correspond to the entire range of the observed spin-down rates ($\dot{E}$) for the MSP and SP.

Goldreich-Julian flux

Broad range of σ values.

Low σ values everywhere applied outside the LC destroy the FF field structure.

We have explored models with low σ only near the open field boundary, extending outside the LC along the current sheet.

FIDO model - Spectral properties

Vela

observations

(Decesar 2013)

model

Phase-resolved spectra

$$\frac{dN}{dE} \propto E^{-\Gamma} e^{-\frac{E}{E_{cut}}}$$

Spectral Index

Cut-off energies

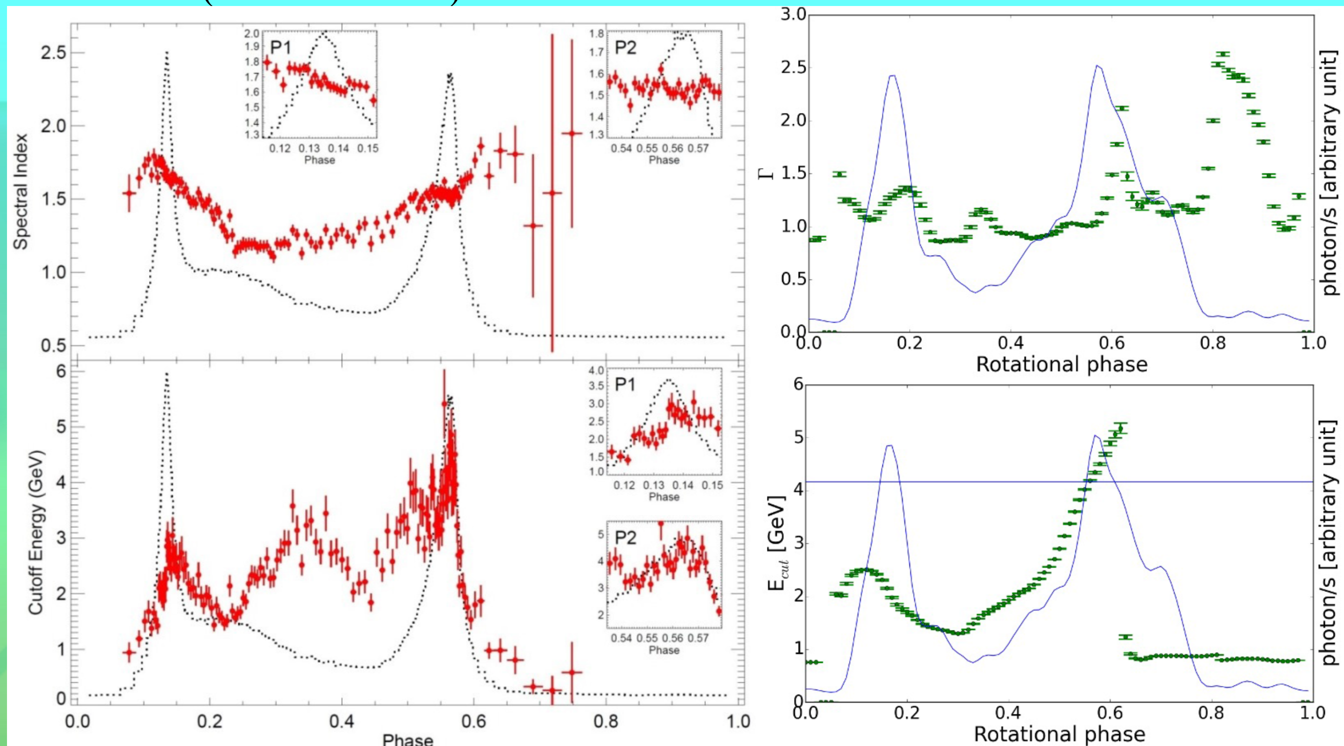

Brambilla et al. 2015

Fitting parameters for Vela

$\alpha = 60°$

$\zeta = 50°$

$\sigma = 10\Omega$

FIDO model - Spectral properties

Vela

observations, 2PC

model

Light-curve energy evolution

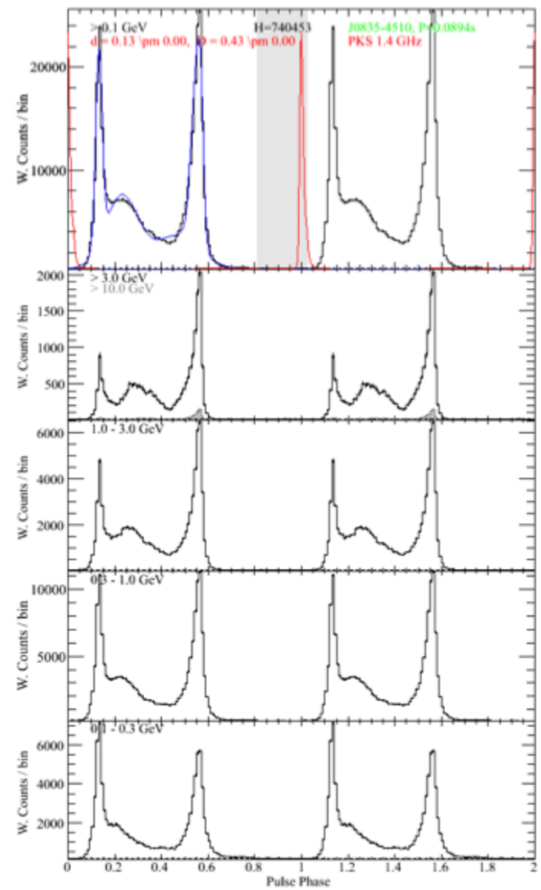

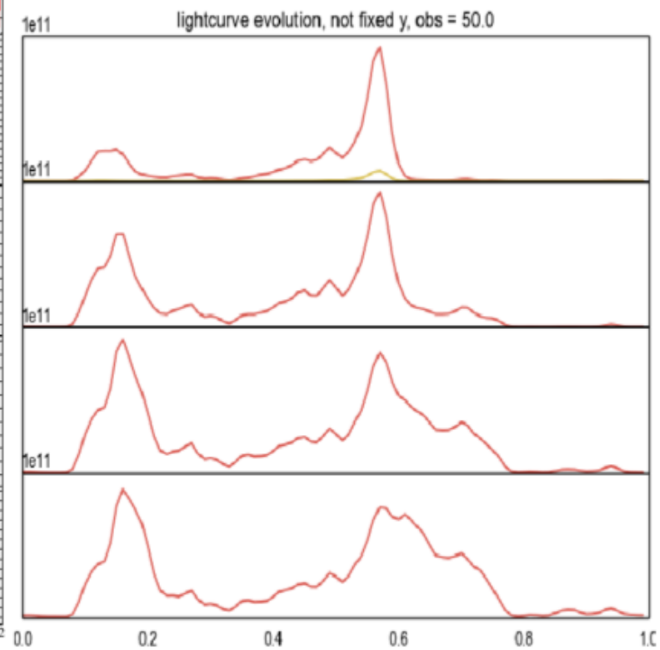

The evolution of the model light-curves with energy is similar to the observed one.

Brambilla et al. 2015

FIDO model - Spectral properties

The results show a significant dependence of L_γ on α.

Is this dependence together with the f_Ω variability with ζ able to explain the observed L_γ scattering?

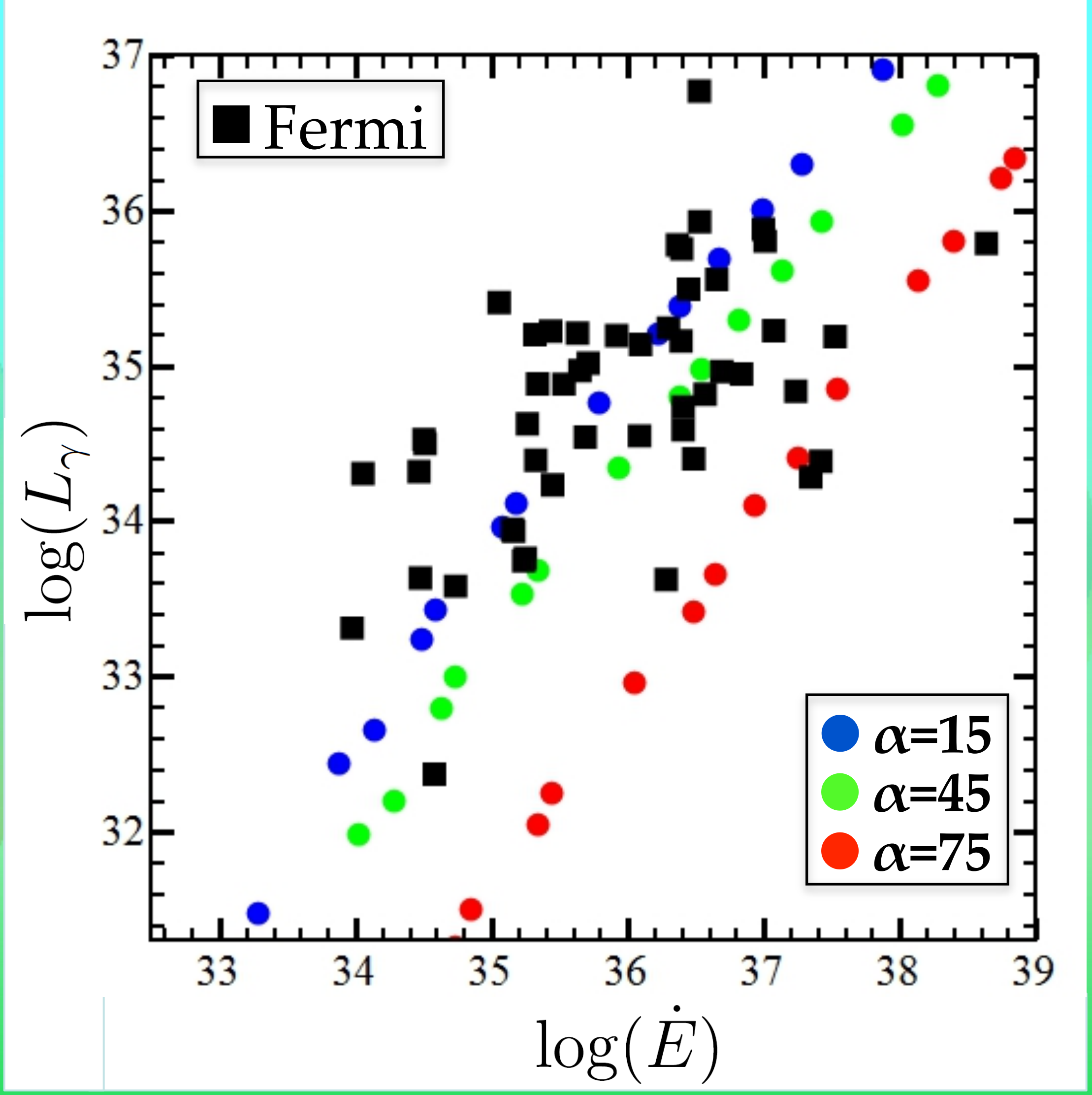

FIDO model - Spectral properties

L_γ is an important property

Is L_γ the most reliable quantity?

L_γ depends on

Observations

- f_Ω **beaming factor**
- α, ζ
- **distance**

Models

- **assumed flux of emitting particles (multiplicity)**

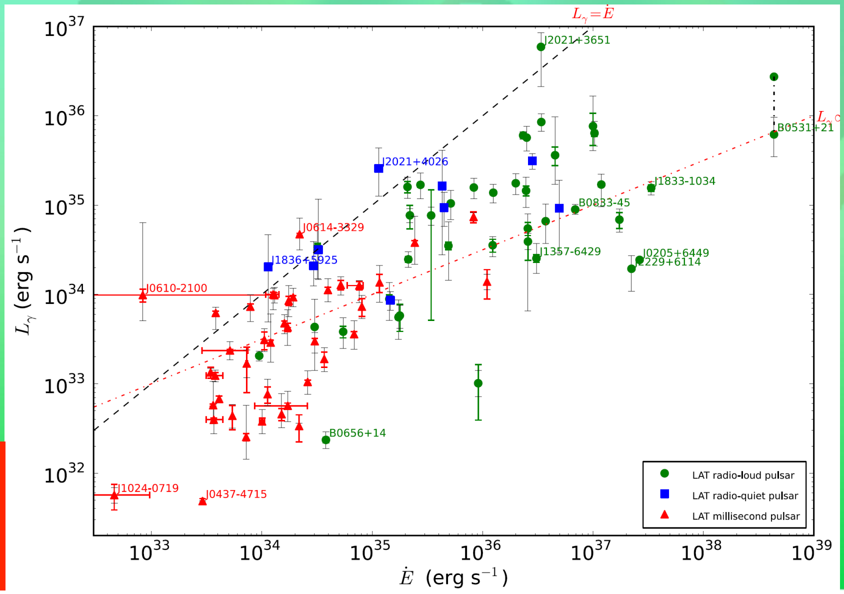

Large scattering
Efficiency 100%

FIDO model - Spectral properties

E_{cut} values are robust and more reliable quantities

They require no further assumptions for their determination

Fermi

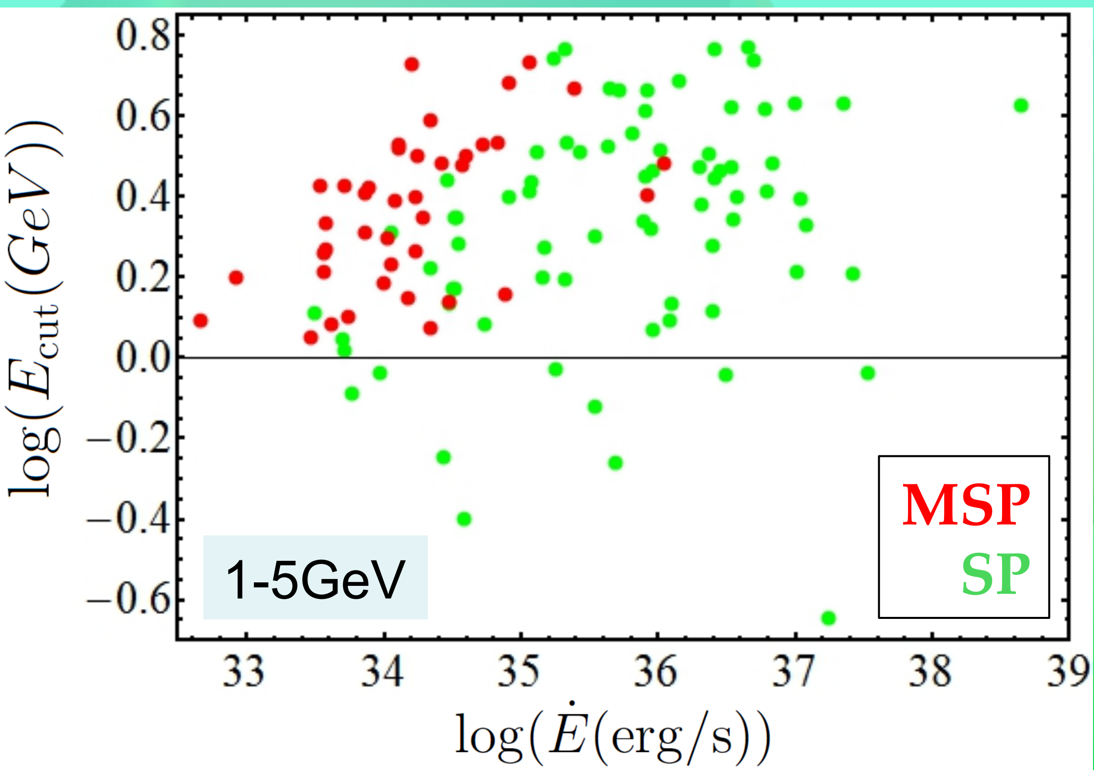

FIDO model - Spectral properties

Fermi E_{cut} values provide a unique insight for the determination of the E_0 (σ).

Radiation Reaction Limit Regime

$$0 = \frac{d\gamma_L}{dt} = \frac{q_e c E_{\parallel}}{m_e c^2} - \frac{2 q_e^2 \gamma_L^4}{3 R_C^2 m_e c}$$

$f\, B_{LC}$

$$E_{\rm cut} = \frac{3}{2} c \hbar \frac{\gamma_L^3}{R_C}$$

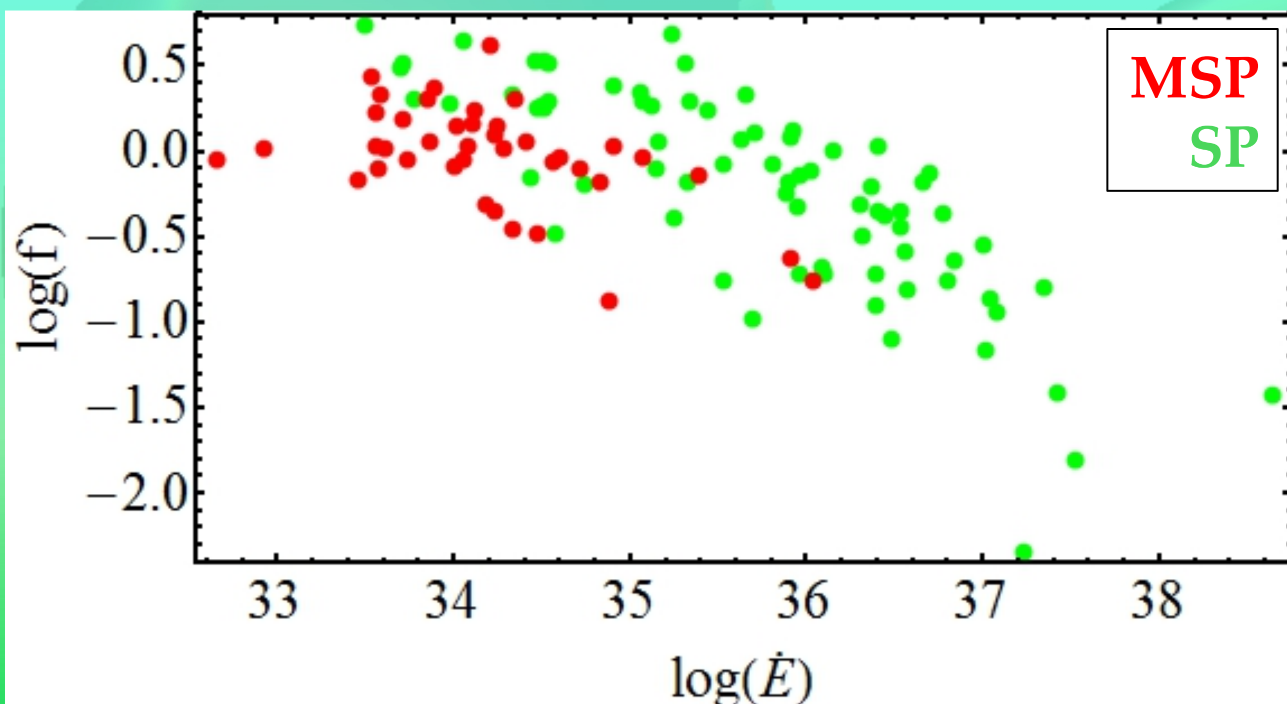

FIDO model - Spectral properties

Fermi

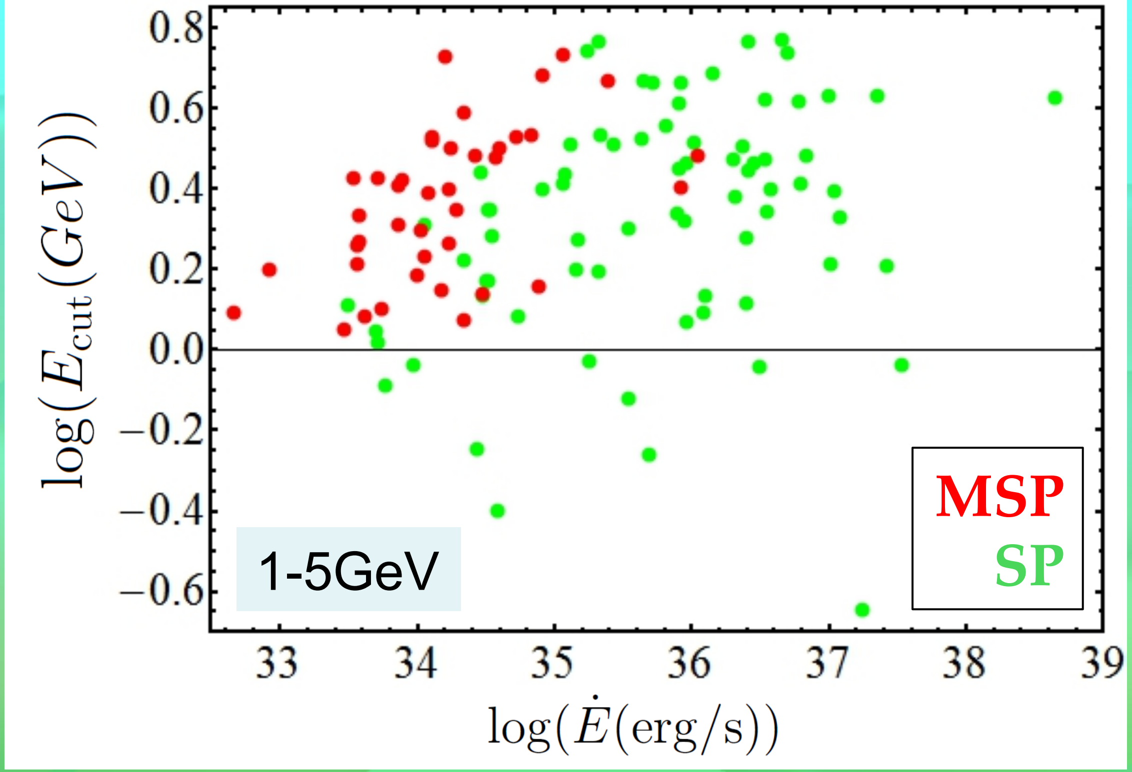

FIDO model - Spectral properties

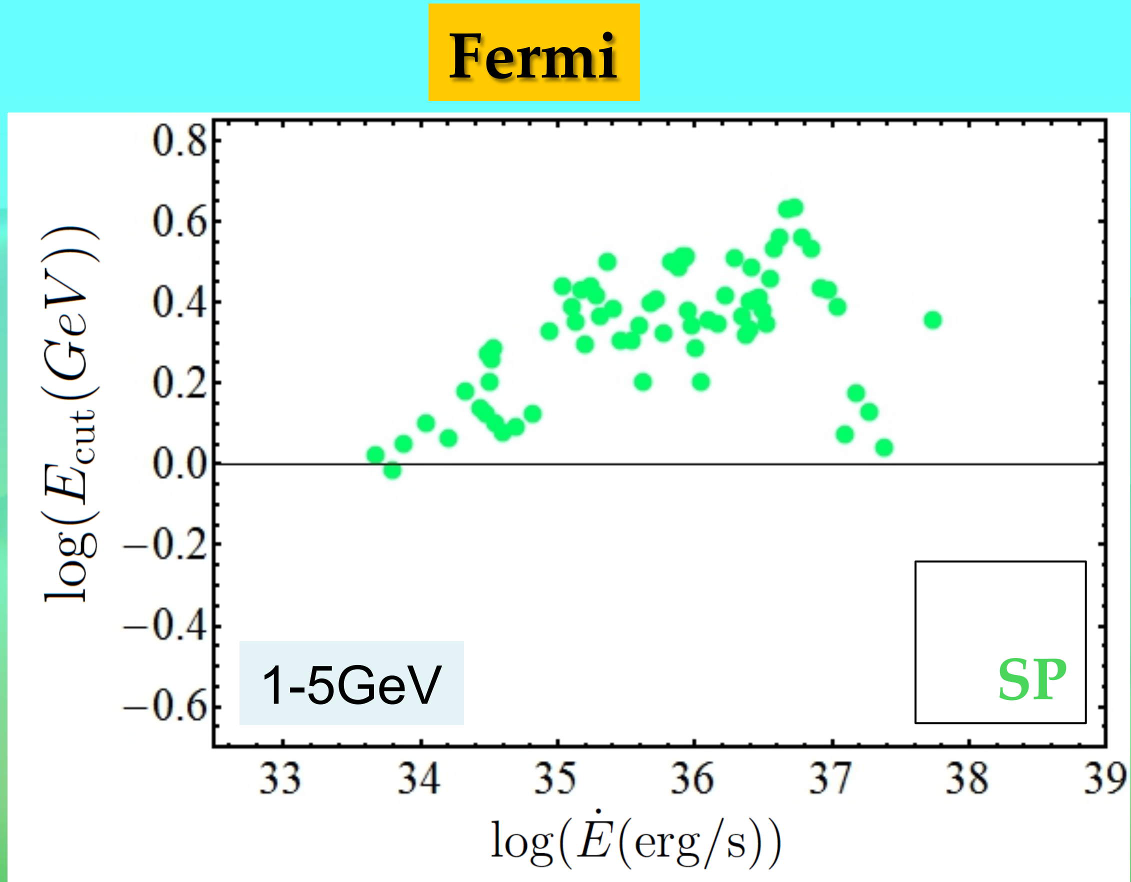

FIDO model - Spectral properties

Fermi

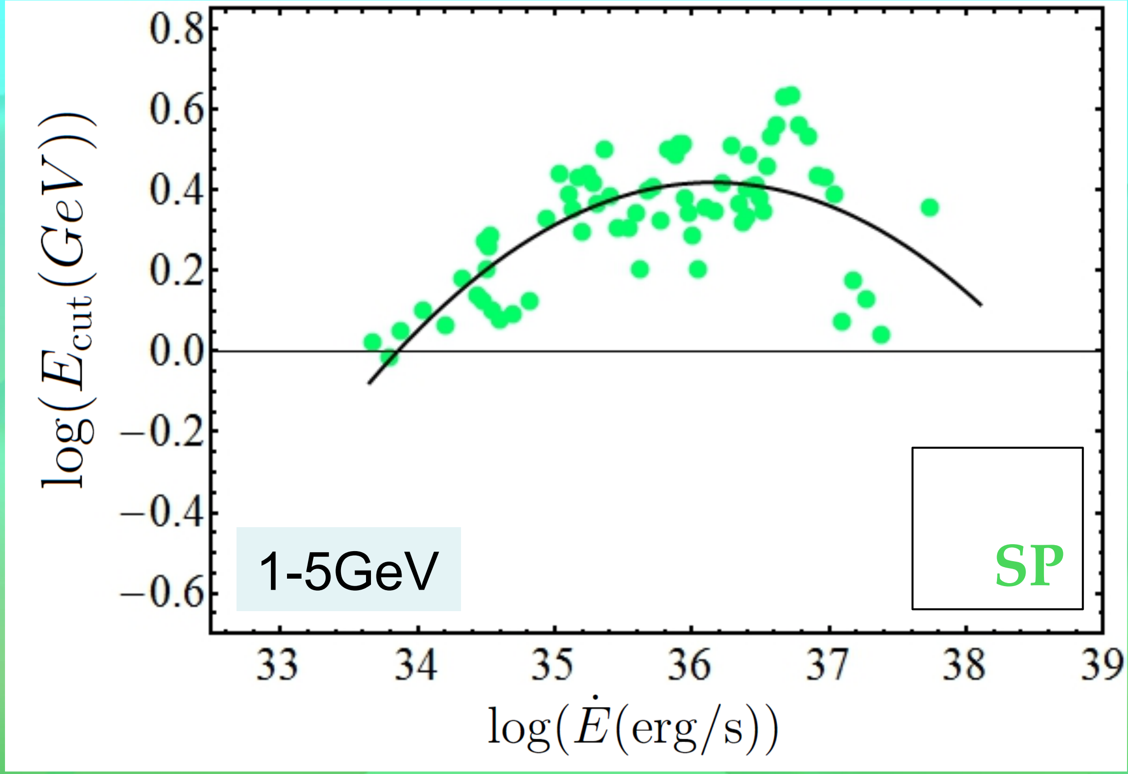

FIDO model - Spectral properties

Fermi

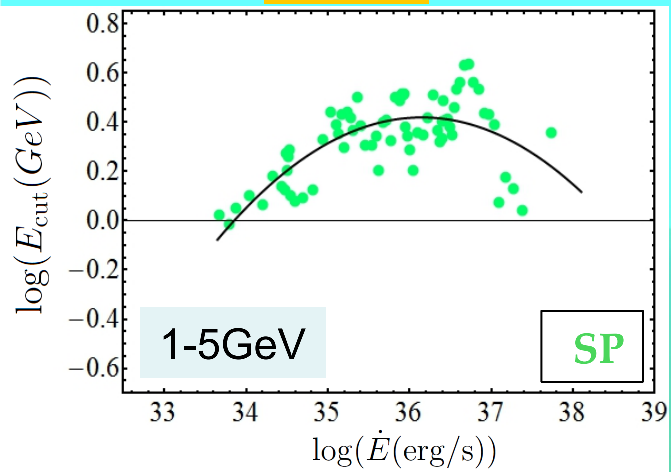

σ vs $\dot{E}$ for SP

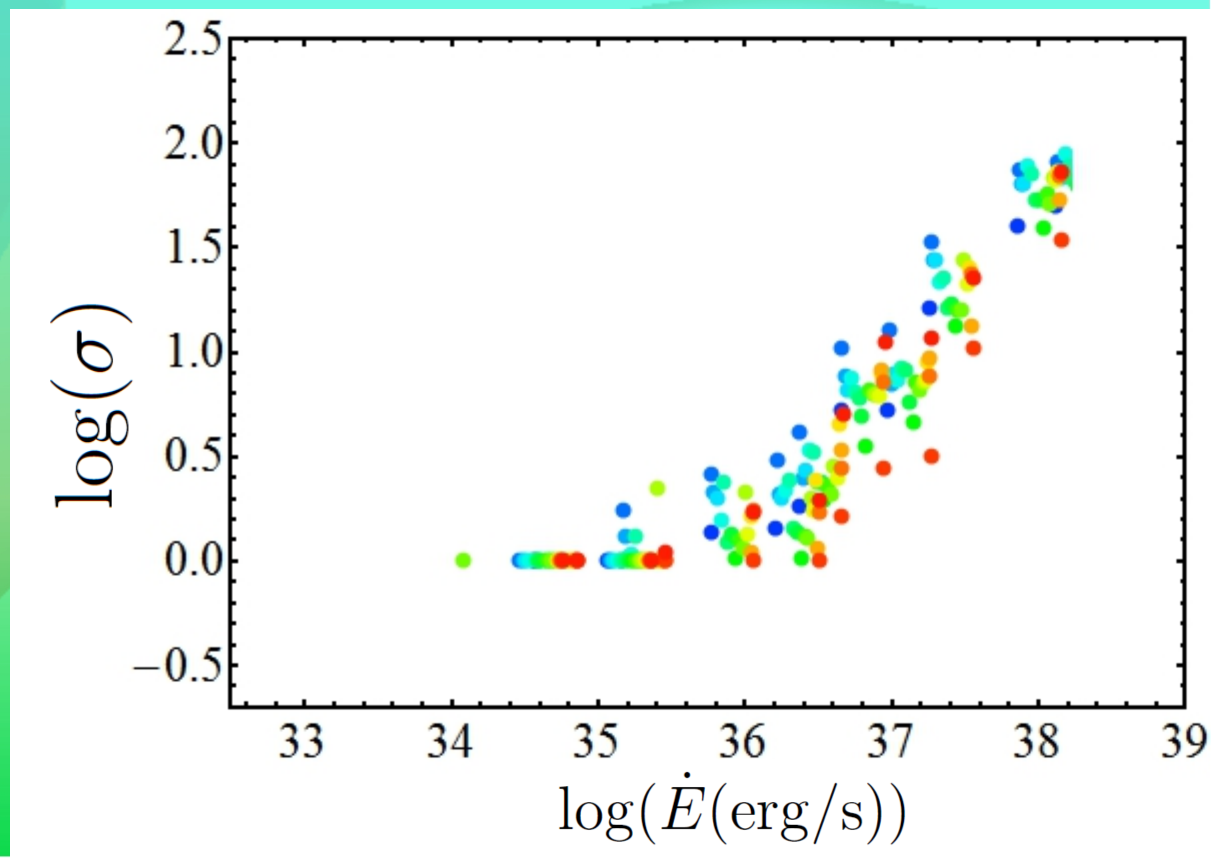

FIDO model - Spectral properties

Fermi

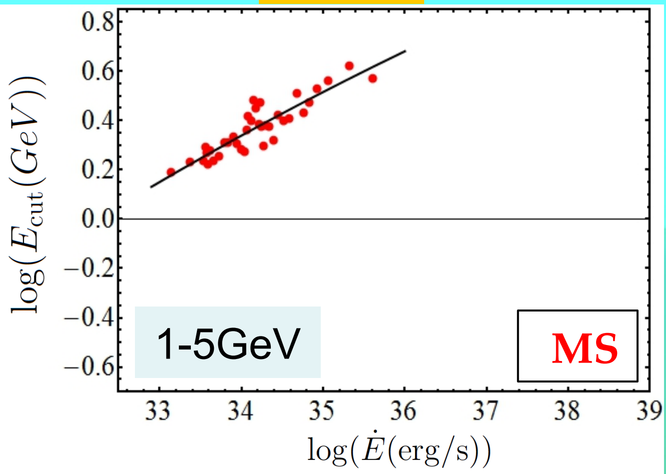

σ vs $\dot{E}$ for MS

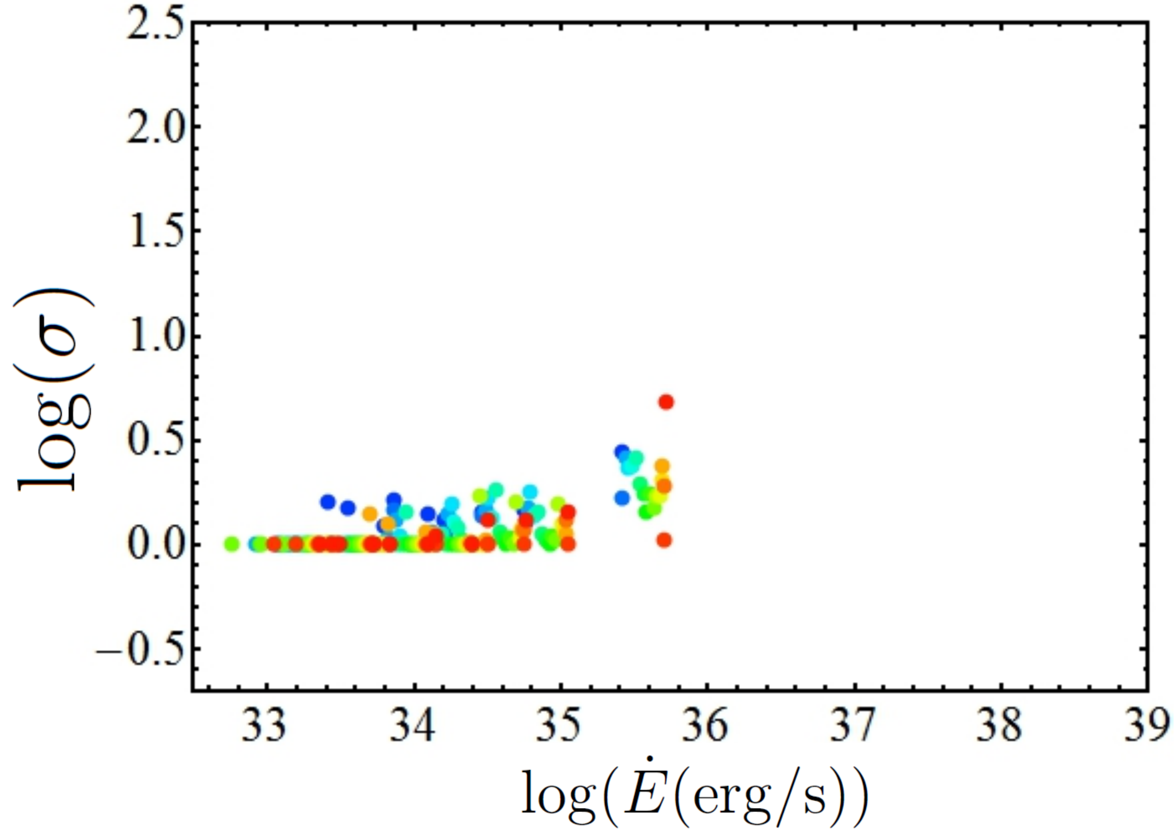

FIDO model - Spectral properties

Fermi

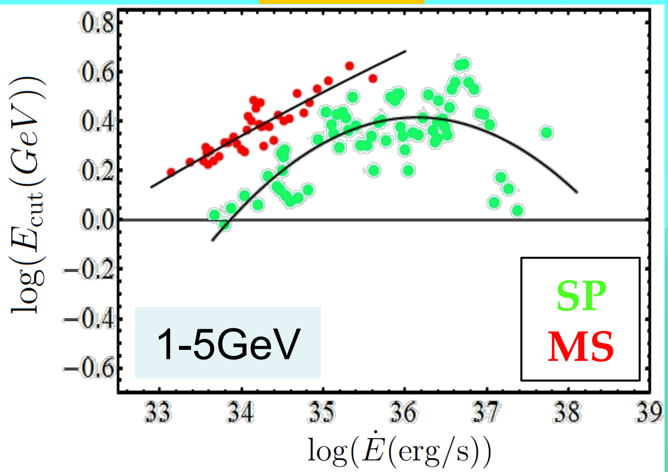

The observed $E_{\rm cut}$ of MS pulsars are slightly higher than those of the SP (for the same $\dot{E}$).

Models show similar behavior.

σ vs $\dot{E}$ for SP & MS

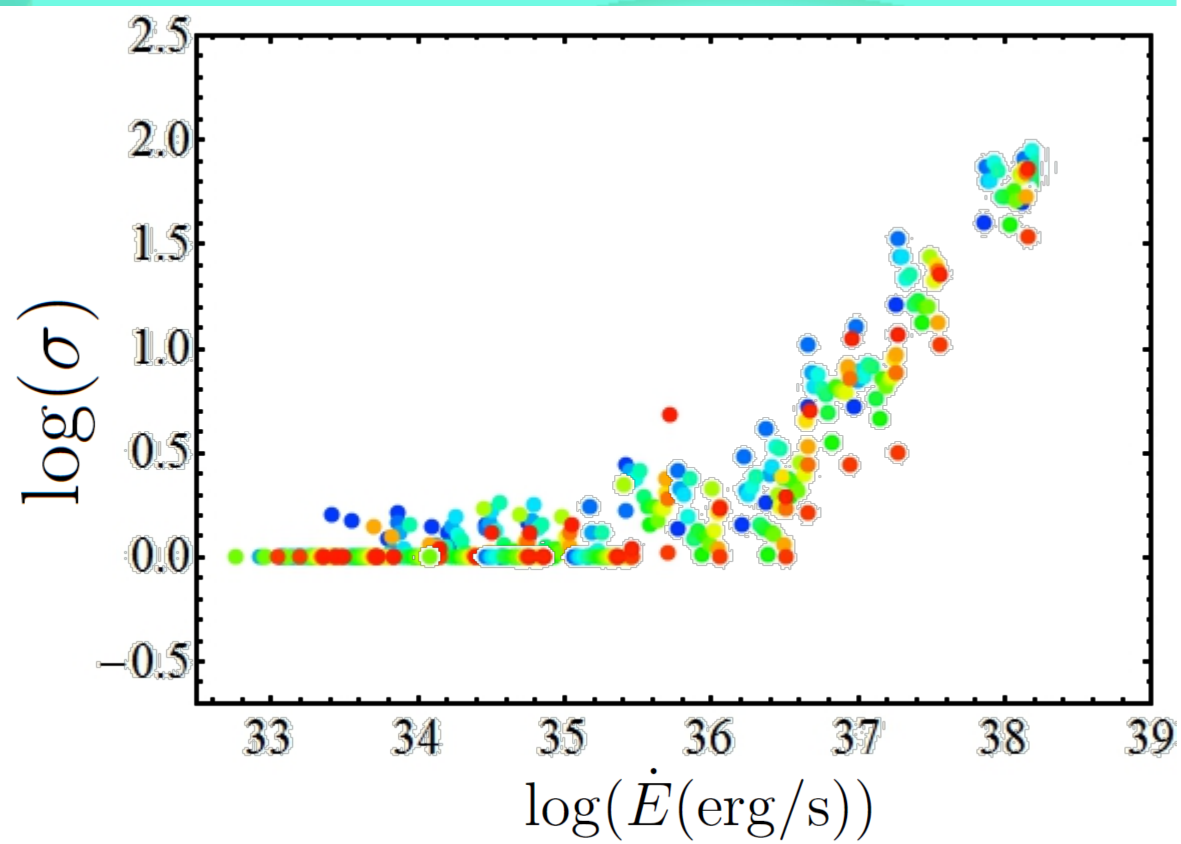

Summary - Future steps

- The γ-ray emission comes from regions near the equatorial <u>current sheet</u>. Simple variable σ model (<u>FFE In –Dissipative Out</u>) reproduces the FERMI phenomenology (<u>light-curves, spectral properties</u>).

Observations
Models – Processes
Success

Eventually, any successful σ distribution should be supported by microphysics.

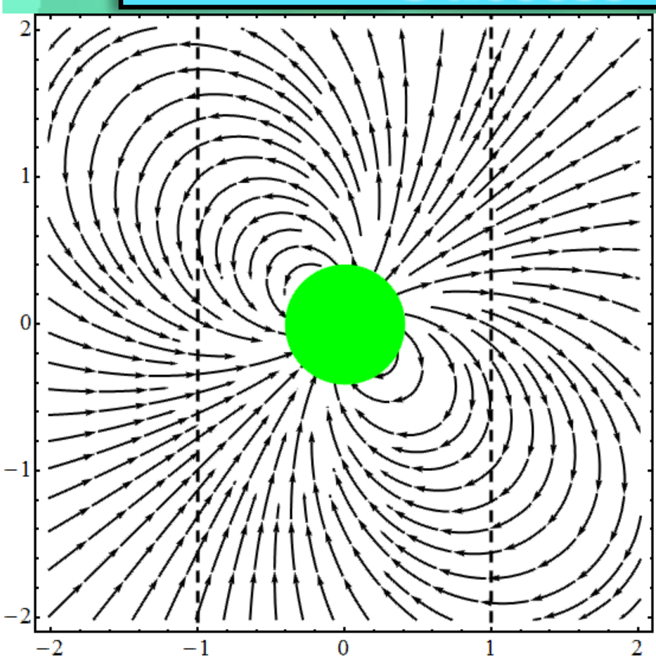

3D PIC code development

Kinetic simulations

Philippov & Spitkovsky 2014
Chen & Beloborodov 2014
Cerutti et al. 2015a,b
Philippov et al. 2015a,b

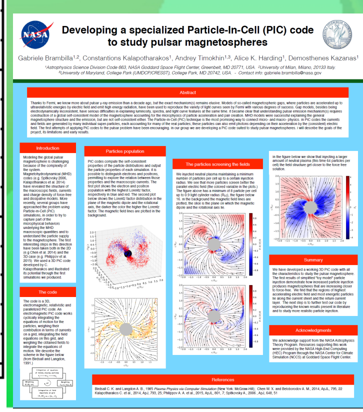

Poster

Brambilla et al.

Summary - Future steps

- The γ-ray emission comes from regions near the equatorial current sheet. Simple variable σ model (FFE In –Dissipative Out) reproduces the FERMI phenomenology (light-curves, spectral properties).

Observations
Models – Processes
Success

Eventually, any successful σ distribution should be supported by microphysics.

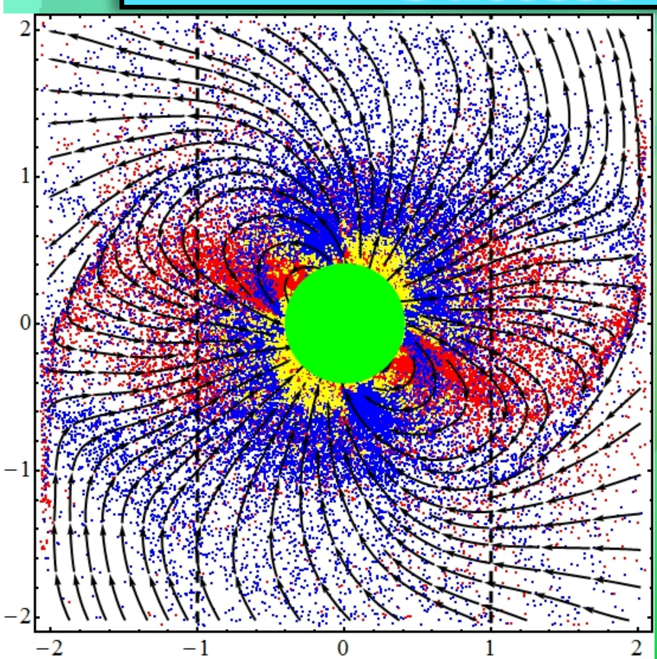

3D PIC code development

Kinetic simulations

macro

micro

observations

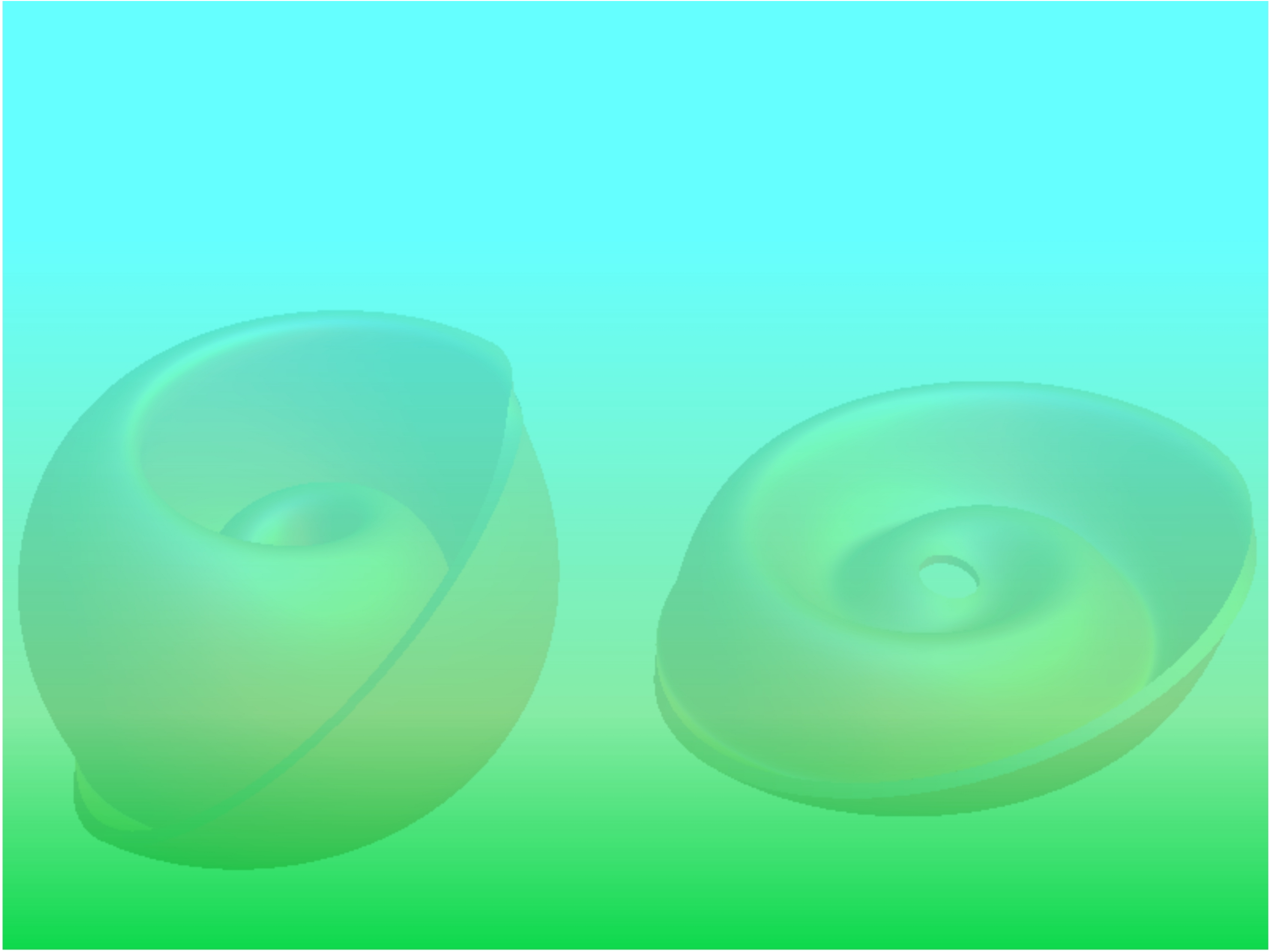

Extras

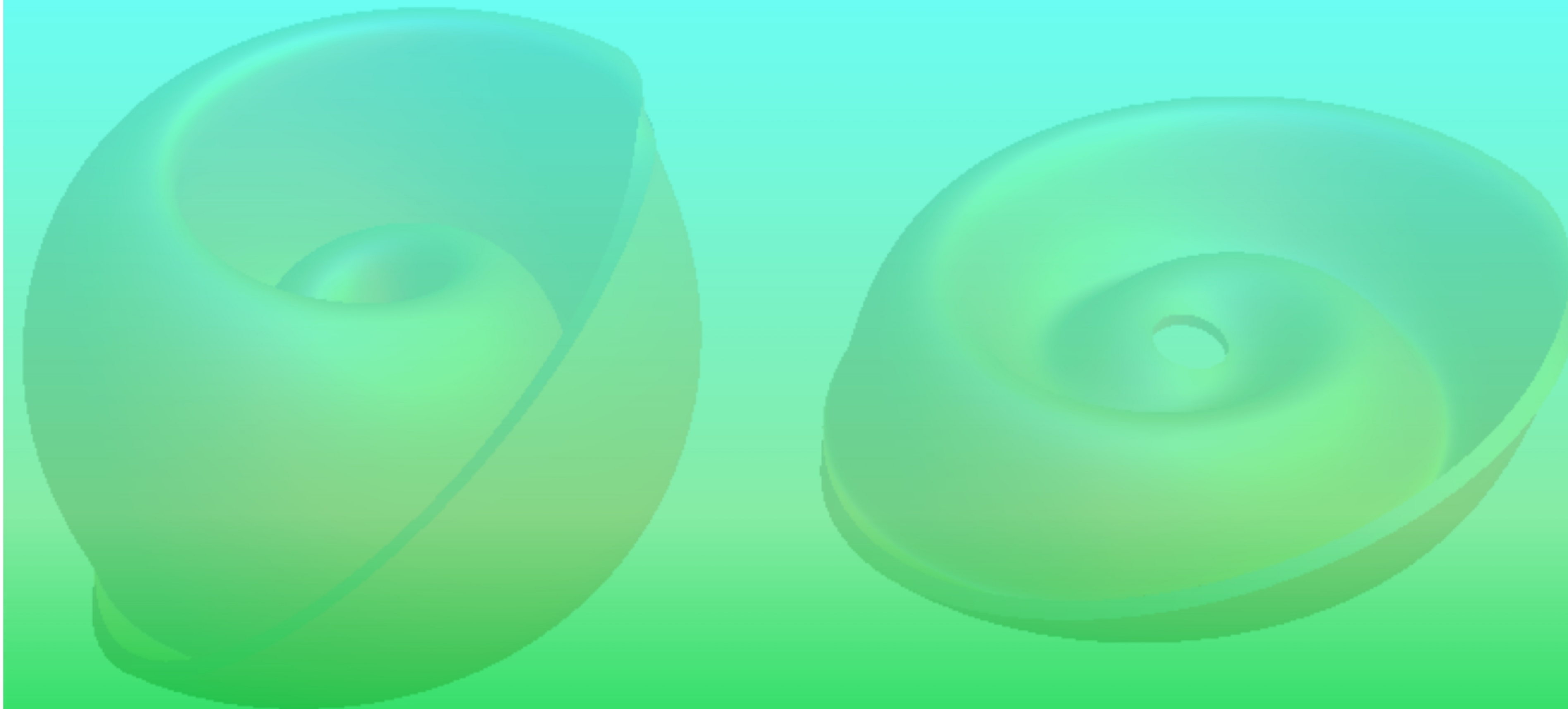

FIDO model - Spectral properties

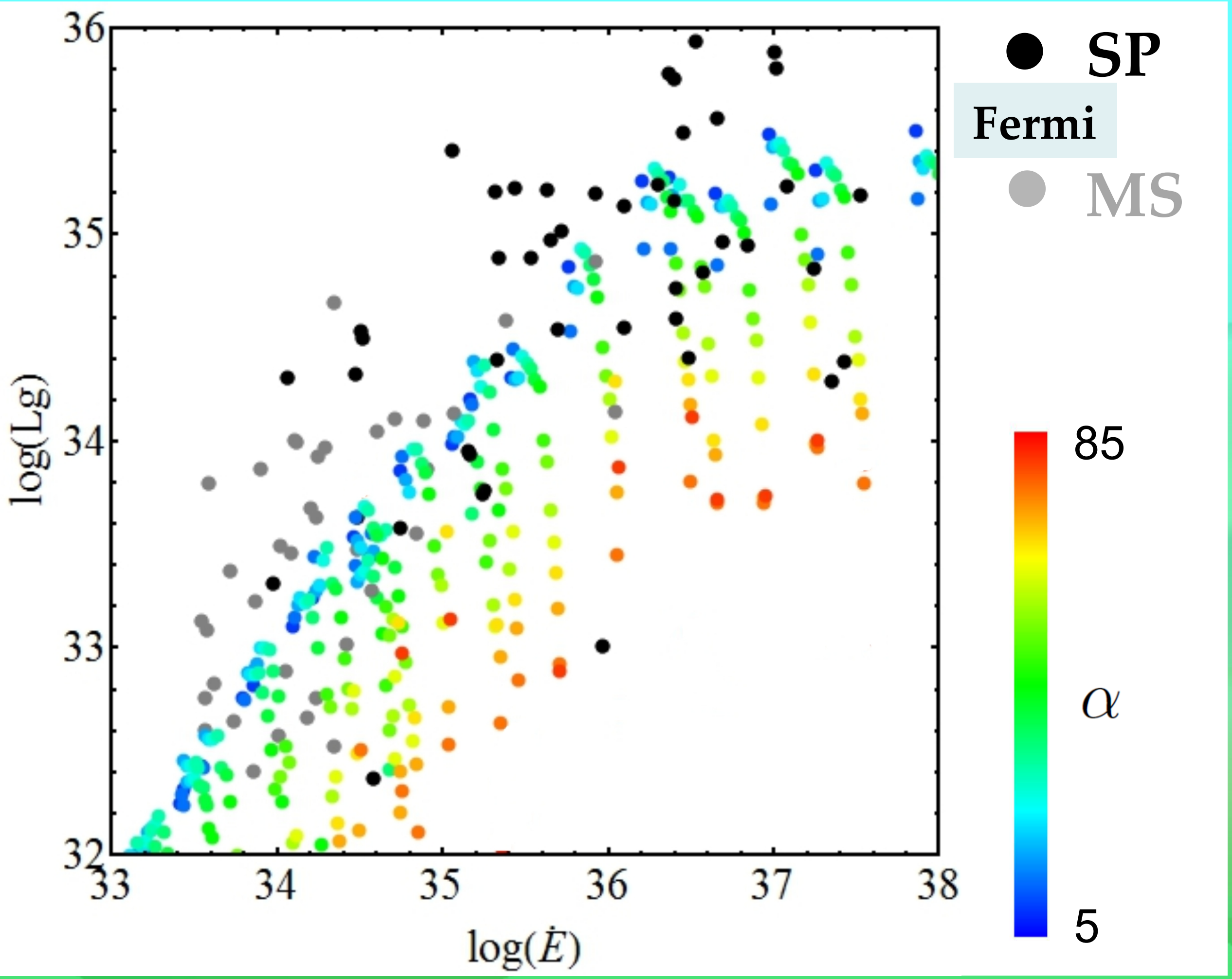

$f_\Omega \approx 0.5$

Multiplicity of the emitting particles

Low $\dot{E}$ → **wider gaps**

High $\dot{E}$ → **higher multiplicity**

Models vs Fermi
light curves

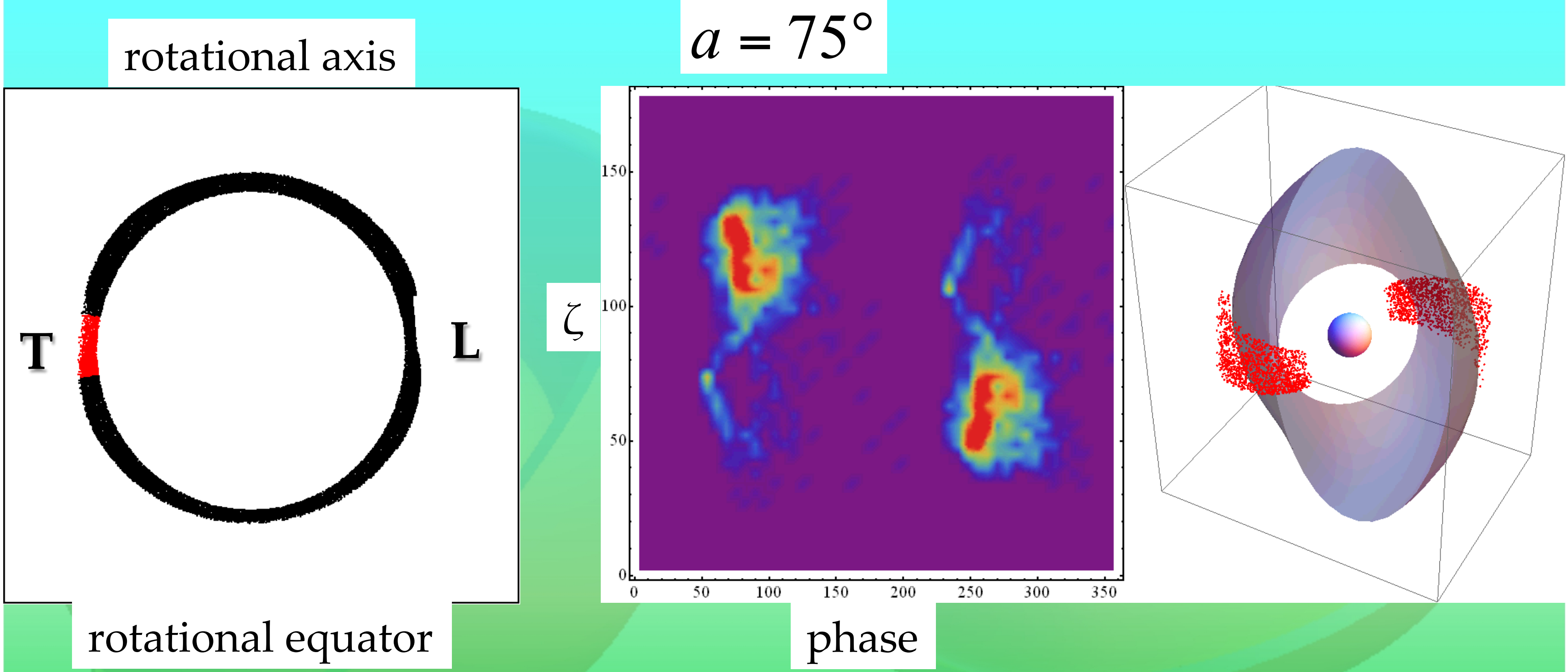

Models vs Fermi
light curves